

PROGRESS REPORT
GRANT NGR 34-002-038/S1

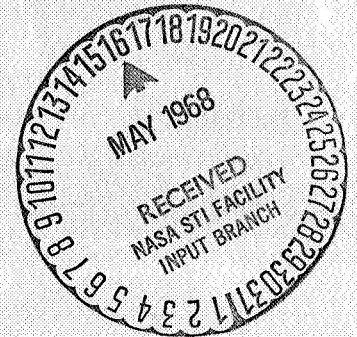
Final Report
on
"NONLINEAR EFFECTS IN OPTICAL
DATA PROCESSING"

J. P. Moffatt
F. J. Tischer

to

The National Aeronautics and Space
Administration, Washington, D. C.

March 15, 1968



NORTH CAROLINA STATE UNIVERSITY
Raleigh, North Carolina

GPO PRICE \$ _____
 CFSTI PRICE(S) \$ _____
 Hard copy (HC) 2.00
 Microfiche (MF) 65.
 ff 653 July 65

N08-22845
 (ACCESSION NUMBER)
85 (PAGES)
94405- (NASA CR OR TAX OR AD NUMBER)
 (THRU) _____
 (CODE) 23
 (CATEGORY)

FACILITY FORM 602

PROGRESS REPORT
GRANT NGR 34-002-038/S1
March 15, 1968

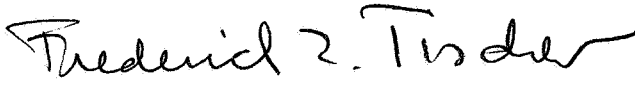
"NONLINEAR EFFECTS IN OPTICAL
DATA PROCESSING"

to

The National Aeronautics and Space
Administration, Washington, D. C.

North Carolina State University
Raleigh, North Carolina

Submitted:



Dr. Frederick J. Tischer, Professor
Principal Investigator

This report is the final form of a paper presenting a study of nonlinear effects in optical data processing. Parts of the study have been discussed previously. The present report not only brings together these parts but also includes results which were obtained during the past two years but were not reported before. It also contains results of specialized investigations which were carried out over an extended period and not completed until recently. The investigation of spectroscopic plates according to methods developed under the grant is an example of such a case. It should be mentioned that the approach developed in this study represents an advance which for the first time facilitates accurate determination of optimum operational conditions for photographic recording. It also allows comparisons to be made of different photographic and other types of recording materials and processors.

ABSTRACT: Methods for the analysis of the effects of nonlinearities in optical data processing are considered. A new method in which nonlinear characteristics are represented by Tchebyscheff's expansions is developed. It is characterized by improved accuracy and simplicity of application. Procedures for the determination of the coefficients and a computer program are described. The procedures and the computer program were used for analysis of spectroscopic photographic plates.

TABLE OF CONTENTS

	Page
LIST OF FIGURES.....	iii
LIST OF TABLES.....	V
1. INTRODUCTION.....	1
2. NONLINEAR EFFECTS.....	6
2.1 Effects of Nonlinearities on Sinusoidal Signals.....	6
2.2 The Description of Nonlinear Effects in Optical Data Processing.....	10
3. NONLINEARITIES IN OPTICAL CORRELATION PROCESSORS....	14
3.1 Mathematical Model of the Operation of an Opti- cal Correlator and Related Reception Systems...	14
3.2 Examples.....	21
4. EXPANSION METHODS FOR DETERMINING HARMONIC COEFFIC- IENTS.....	29
4.1 Introduction.....	29
4.2 Taylor Series.....	31
4.3 Fourier Series - Method A.....	33
4.4 Fourier Series - Method B.....	36
4.5 Legendre Series.....	38
4.6 Tchebyscheff Series.....	41
4.7 Relative Advantages.....	43
5. COMPARISON OF THE EXPANSION METHODS.....	44
6. A NUMERICAL METHOD FOR COMPUTING TCHEBYSCHIEFF COEFFIC- IENTS.....	49
7. A FORTRAN PROGRAM FOR COMPUTING HARMONIC COEFFICIENTS AND NOISE-TO-SIGNAL RATIOS.....	55
8. ANALYSIS OF THE CHARACTERISTIC CURVES OF TYPE 649-F SPECTROSCOPIC PLATES.....	59
9. CONCLUSIONS AND RESULTS.....	70
10. REFERENCES.....	72
11. COMPUTER PROGRAM.....	74

LIST OF FIGURES

	Page
1. Effects of a Nonlinear characteristic on a sinusoid..	7
2. A linear characteristic.....	23
3. A square law characteristic.....	23
4. An exponential characteristic.....	24
5. Typical "high-gamma" characteristic normalized to [-1,1].....	45
6. Approximations to the harmonic coefficient b_1	47
7. Approximations to the harmonic coefficient b_2	47
8. Approximations to the harmonic coefficient b_3	48
9. Approximations to the harmonic coefficient b_4	48
10. Typical characteristic and desired expansion region..	51
11. A piecewise linear approximation to the character- istic.....	51
12. Flow chart for the program ODP-11.....	58
13. Characteristic curves for type 649-F spectroscopic plates.....	60
14. Output fundamental amplitudes for the 2 minute char- acteristic.....	62
15. Output fundamental amplitudes for the 3 minute char- acteristic.....	63
16. Output fundamental amplitudes for the 5 minute char- acteristic.....	64
17. Output fundamental amplitudes for the 9 minute char- acteristic.....	65
18. Noise-to-signal ratios for the 2 minute character- istic.....	66
19. Noise-to-signal ratios for the 3 minute character- istic.....	67
20. Noise-to-signal ratios for the 5 minute character- istic.....	68

LIST OF FIGURES (Continued)

	Page
21. Noise-to-signal ratios for the 9 minute characteristic.....	69
22. Optimum noise-to-signal ratios for the 649-F characteristic curves.....	71

LIST OF TABLES

	Page
Table 1. Error-power ratios corresponding to three optical recording characteristics.....	26

1. INTRODUCTION

One of the outstanding features of photographic and other optical recording processes is their nonlinearity. In optical data processing, nonlinear effects introduce error signals of various kinds which in some cases such as the detection of signals in noise may reduce the signal-to-noise ratio considerably and seriously limit its practical application. In holography, nonlinearities generate ghost images which interfere with weak signals.

Two general approaches have been used for the analysis of nonlinear effects in optical data processing and holography. In the first, methods suitable for arbitrary or fairly general signals have been employed. Among these are the method as used by Davenport and Root (1958), in which the functional form of the nonlinearity is used directly, and the Fourier Transform method described by Middleton (1960). Use of these methods, however, has been confined to rather simple forms of nonlinear characteristics. Many characteristics, however, do not have such simple forms. When these methods are applied to more complicated or realistic characteristics, the resulting equations usually become exceedingly involved.

In the second general approach, the class of signals, for which the nonlinear effects are obtained, has been restricted to sinusoids. By doing this, the analysis can be extended to more realistic characteristics without excessive

complications. Methods following this approach have been primarily based on the Taylor Series expansion. An early description of a version of this expansion method was given by Espley (1933) and more recent references include Ryder (1964) and Chirlian (1965).

In the literature on optical data processing and holography, the first approach has been used by Kozma (1966) and Friesem and Zelenka (1967). Kozma employed an error-function-limiter form of the characteristic for nonlinearities in photographic recording processes. This model demonstrated the presence of amplitude and phase distortions in recorded signals. Friesem and Zelenka assumed an odd power-law model of the form

$$f(x) = x |x|^{\nu-1},$$

where $\nu \geq 0$, for describing photographic recording in holography. The resulting nonlinear effects were shown to cause "ghost" images to appear in the reconstruction of scenes containing point sources.

Literature on the second approach has dealt with two applications. In the first, photographic nonlinearities have been described by the so-called gamma-law model. This method has been used by Lamberts (1961) and Little (1966). Lamberts derived expressions for the harmonic distortion of recorded sinusoidal exposure patterns, assuming such a model. Little demonstrated that these distortions can be

minimized in positive photographic processes by proper adjustment of exposure conditions and development times. This second paper, however, includes experimental results which show nonsatisfactory agreement between the harmonics obtained from the gamma-law model and from actual photographic processes.

The second application of the sinusoidal signal approach has been developed by Wilczynski (1961). In this method, the Taylor Series expansion is applied directly to the characteristic curve of the photographic process under investigation and the harmonics of recorded sinusoidal exposure patterns are obtained from the expansion. Wilczynski applied this method to the characteristic curves of Ilford chromatic plates and was able to calculate the harmonics obtained from a wide range of exposure conditions and development times. In most instances, the calculations agreed quite well with accompanying experimental measurements.

The present investigation was begun as an extension of Wilczynski's approach. Taylor series expansions were employed along with curve-fitting procedures for evaluating the expansion coefficients. During the application of this method, difficulties were encountered in accurately representing the characteristics of photographic processes. This led to a study of expansion methods. Use of the Tchebyscheff expansion was suggested for this purpose (Tischer, 1967) and subsequently employed. Theoretical and experimental results

showed this method to have advantages over the Taylor series both in accuracy and ease of application.

In the following considerations, the effects of nonlinearities on sinusoidal signals are first described in a general manner. The nonlinearities are shown to create harmonic distortions of the signals. An equivalent noise-to-signal ratio (NSR) is introduced next. It describes the degree of distortion by a single figure. The consequences of these distortions on the operation of an idealized optical correlator are then described. Specific examples demonstrate the resulting degraded performance.

Methods for determining the harmonic coefficients of distorted signals are then developed. Taylor, Legendre, Tchebyscheff, and Fourier expansions are considered for this purpose. In many applications, the expansions must be truncated. The consequences of truncation are investigated. The results show the advantages of the Tchebyscheff method.

The remainder of the report deals with the application of the Tchebyscheff method to actual nonlinear problems. A numerical method for obtaining the Tchebyscheff coefficients from nonlinear characteristics is developed first. This method is subsequently implemented in a Fortran program. The program facilitates the comparison of nonlinear characteristics by computing the harmonic coefficients and noise-to-signal ratios. It also allows determination of operational

conditions under which the nonlinear effects of a specific characteristic are minimized. The program is then used to analyze the nonlinearities of type 649-F spectroscopic plates which are widely employed in optical data processing and holography.

It should be mentioned that application of the described method of analysis is not limited to optical recording but can also be used for the investigation of other processes where signals are transmitted through components having nonlinear characteristics.

2. NONLINEAR EFFECTS

2.1 Effects of Nonlinearities on Sinusoidal Signals

The amplitude behavior of a (zero-memory) device having a nonlinear functional relation between its input and output variables may be represented in terms of a characteristic curve such as that shown in Fig. 1. The curve relates the output variable y to the input variable x and is a graph of the transfer function

$$y = f(x). \quad (1)$$

If the input variable consists of a signal varying about some value x_0 , which is called the operating point of the device, then

$$S_1(t) = x - x_0, \quad (2)$$

where $S_1(t)$ represents the input signal which is a function of some other variable t . In general, the operating point of the device may be chosen anywhere on the characteristic. The form of the output signal thus depends on the location of the operating point as well as the input signal. The output can thus be represented by

$$S_2[S_1(t), x_0] = y - y_0, \quad (3)$$

where S_2 represents the output signal, and y_0 corresponds to the output of the device at the operating point. Substitution of Eqs. (1) and (2) into the right hand side of Eq. (3) yields

$$S_2[S_2(t), x_0] = f[S_1(t) + x_0] - y_0. \quad (4)$$

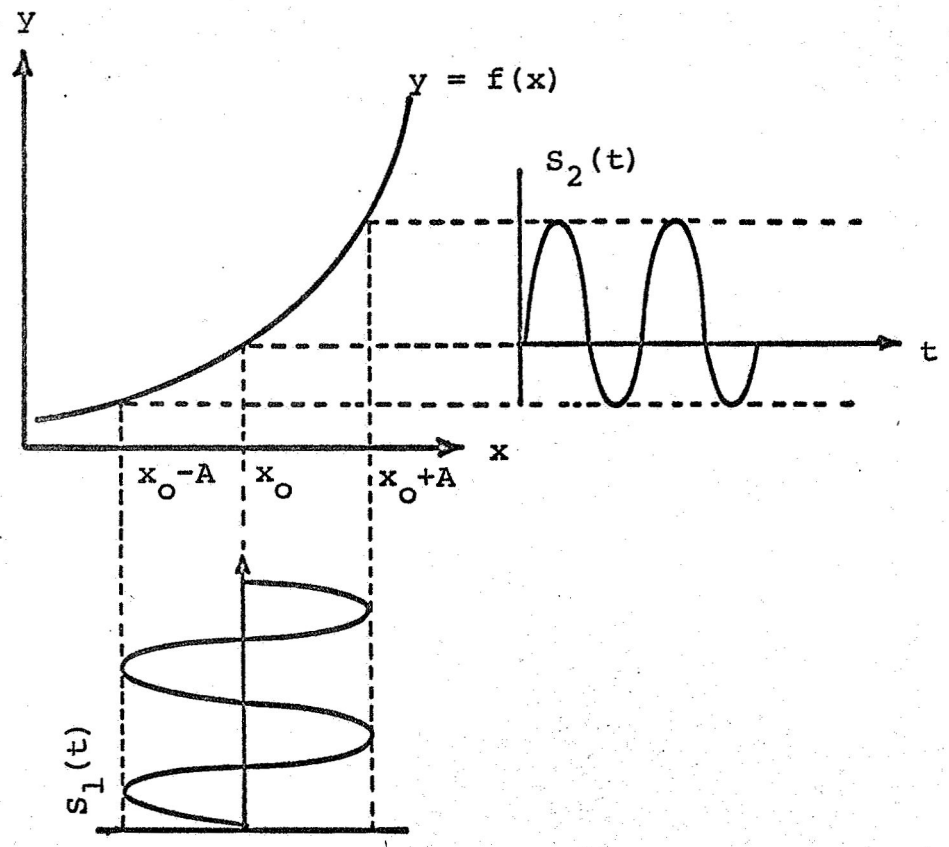


Figure 1. Effects of a nonlinear characteristic on a sinusoid

If $S_1(t)$ is an arbitrary sinusoidal signal given by

$$S_1(t) = A \cos(\omega t + \phi), \quad (5)$$

where A is the amplitude of the signal, ω is its radian frequency, and ϕ is its phase at $t = 0$, Eq. (4) may be written

$$S_2(t, A, x_0) = f[A \cos(\omega t + \phi) + x_0] - y_0, \quad (6)$$

where the dependence of S_2 on ω and ϕ is understood. The functional form of S_2 then depends on both the operating point and the amplitude of the sinusoidal input. Equation (6) shows that

$$S_2\left(t + \frac{2\pi}{\omega}, A, x_0\right) = S_2(A, t, x_0). \quad (7)$$

The function S_2 , thus, is periodic in t with fundamental radian frequency ω . If the function f is piecewise continuous, S_2 can be expressed by a convergent Fourier series in t . The series can be written as

$$S_2(t, A, x_0) = \frac{b_0(A, x_0)}{2} + \sum_{n=1}^{\infty} b_n(A, x_0) \cos[n\omega t + \phi_n(A, x_0)], \quad (8)$$

where b_n and ϕ_n represent respectively the amplitude and phase of the n^{th} harmonic.

Additional information about S_2 may be obtained by letting

$$(\omega t + \phi) = \theta, \quad (9)$$

in Eq. (5). Eq. (6) becomes

$$S_2(\theta, A, x_0) = f[A \cos \theta + x_0] - y_0 \quad (10)$$

Thus

$$S_2(-\theta, A, x_0) = S_2(\theta, A, x_0), \quad (11)$$

showing that S_2 is an even function in θ . The Fourier series expansion of $S_2(\theta, A, x_0)$, in θ , then contains only terms of the type $\cos(n\theta)$. Comparing this to Eq. (8) shows

$$n\theta = n(\omega t + \phi) = n\omega t + n\phi, \quad (12)$$

or

$$\phi_n = n\phi. \quad (13)$$

Thus, the phase shifts of the various harmonics of Eq. (8) do not depend on A , x_0 , or the functional form of $f(x)$. This series can then be written as

$$S_2(t, A, x_0) = \frac{b_0(A, x_0)}{2} + \sum_{n=1}^{\infty} b_n(A, x_0) \cos[n(\omega t + \phi)]. \quad (14)$$

The effects of the nonlinearity of $f(x)$ on the input sinusoid are apparent in this expression. The term $b_1 \cos(\omega t + \phi)$ corresponds to the input S_1 . The device introduces no phase shift in this signal. The term $b_0/2$ corresponds to a D. C. bias and the various terms $b_n \cos[n(\omega t + \phi)]$ correspond to harmonic distortions of S_1 . The nonlinearity produces no subharmonics of the input sinusoid. This effect occurs only when the input consists of more than one frequency.

Equation (14) indicates the dependence of the harmonic coefficients on the operating point of the nonlinear device x_0 , and the amplitude of the sinusoidal signal A . If such a device is used in a system where linearity is desired, knowledge of the dependence of these coefficients on x_0 and A would show quantitatively the nonlinear effects and reveal

optimum input conditions for their minimization. Subsequent sections present methods of obtaining these coefficients from characteristic curves.

2.2 The Description of Nonlinear Effects in Optical Data Processing

In the previous section, a device having a nonlinear characteristic was shown to create distortions of an input sinusoid. For a signal given by

$$S_1(t) = A \cos(\omega t) \quad (15)$$

the output of the device was described by

$$S_2(t) = \frac{b_0}{2} + \sum_{n=1}^{\infty} b_n \cos(n\omega t), \quad (16)$$

where the b coefficients depend on the amplitude of the input sinusoid A and the operating point of the device. A complete description of the nonlinear effects consists of specifying these coefficients. In many instances, however, a complete description of the effects is not needed, and a single quantity describing their severity is sufficient.

In electronic circuit theory a quantity called the "total harmonic distortion" is used for describing the effects of nonlinearities on sinusoidal signals (Ryder, 1964). For a distorted sinusoid, this quantity is given by the ratio of the r.m.s. value of the sum of the harmonics to that of the fundamental. In terms of Eq. (16), it becomes

$$D = \frac{\left[\sum_{n=2}^{\infty} b_n^2 \right]^{1/2}}{b_1}. \quad (17)$$

The square of this quantity given by

$$D^2 = \frac{\sum_{n=2}^{\infty} b_n^2}{b_1^2}, \quad (18)$$

represents the ratio of the total power carried by the harmonics to that of the fundamental. If the harmonics are considered as an equivalent noise generated by the nonlinearity, Eq. (18) is equivalent to the reciprocal of the well-known signal-to-noise power ratio of communication theory (Schwartz, 1959, p. 226). The term equivalent noise is used to describe the harmonics here since the usual communication theory definition of noise assumes that it is independent of the signal. The harmonics generated by nonlinearities are signal dependent and cannot strictly be called noise. The signal-to-noise ratio is defined by

$$SNR = \frac{P_s}{P_n}, \quad (19)$$

where P_s is the signal power and P_n is the noise power.

Eq. (18) thus represents an equivalent noise-to-signal ratio or

$$NSR = \frac{P_n}{P_s} = \frac{\sum_{n=2}^{\infty} b_n^2}{b_1^2}. \quad (20)$$

Two other quantities expressing nonlinear effects in terms of signal and equivalent noise power are defined as the "signal-power fraction"

$$SPF = \frac{P_s}{P_s + P_n}, \quad (21)$$

and the "noise-power fraction"

$$NPF = \frac{P_n}{P_s + P_n}. \quad (22)$$

In terms of the harmonic coefficients, these become

$$SPF = \frac{b_1^2}{\sum_{n=1}^{M} b_n^2}, \quad (23)$$

and

$$NPF = \frac{\sum_{n=2}^{M} b_n^2}{\sum_{n=1}^{M} b_n^2}. \quad (24)$$

All of these descriptions of nonlinear effects are equivalent in that they are functionally related. The knowledge of any one permits the calculation of the others without additional information.

In optical data processing systems, multiple noise sources can exist. For example, photographic processes, in addition to being nonlinear, contain fluctuations in image structure known as granularity. This effect can be considered as the addition of noise to the image. If such a process is to be fully evaluated, both effects must be considered. For this reason, the amenability of the above quantities to include additional noise sources was investigated. Two sources, having equivalent noise powers given by N_1 and N_2 were assumed. The noise N_1 gives rise to D_1 , NSR_1 , SNR_1 , and NPF_1 , while N_2 produces D_2 , NSR_2 , SNR_2 , SPF_2 , and NPF_2 . The addition of the two sources gives rise to the following expressions for the combined quantities

$$D = \sqrt{D_1^2 + D_2^2}, \quad (25)$$

$$NSR = NSR_1 + NSR_2, \quad (26)$$

$$SNR = \frac{(SNR_1)(SNR_2)}{SNR_1 + SNR_2} , \quad (27)$$

$$SPF = \frac{(SPF_1)(SPF_2)}{SPF_1 + SPF_2 - (SPF_1)(SPF_2)} , \quad (28)$$

$$NPF = \frac{NPF_1 + NPF_2 - 2(NPF_1)(NPF_2)}{1 - 3(NPF_1)(NPF_2)} . \quad (29)$$

These equations show that the quantity NSR is most easily calculated when two sources are present. The simple addition rule indicated by Eq. (26) can be extended to include multiple sources. For these reasons, the NSR description of nonlinear effects was chosen for use in subsequent work.

3. NONLINEARITIES IN OPTICAL CORRELATION PROCESSORS

In this section, the effects of nonlinearities on the operation of a typical optical correlator are described. The correlator is assumed to operate as part of a larger electronic system for the reception of pulse-frequency modulation telemetry. The reception system (Rochelle, 1963) is used in satellite and space probe communications. Optical recording processes are assumed to transform the electrical signals into photographic transparencies which form the input to the correlator. These processes can contain nonlinearities which degrade the correlator operation. A description of the reception system and an idealized model of its operation with linear recording processes are first presented. Nonlinearities in the optical recording are then introduced and the resulting effects on the correlation processing described. Finally, three numerical examples are presented. In these, typical optical recording characteristics are used to demonstrate quantitative effects on the correlator operation.

3.1 Mathematical Model of the Operation of an Optical Correlator and Related Reception System

The reception system receives a sequence of frequency modulated RF pulses. The pulses are of time-length T and begin at intervals of $2T$. During each pulse, a single RF frequency is transmitted. This frequency corresponds to one of a set of N possible signals. The detection process consists of determining which of these signals is present in

each pulse. Previous to the correlation processing, the RF pulses are demodulated to form a sequence of low-frequency, time-limited sinusoids. The sinusoids corresponding to the various signals are harmonically related. A member of the demodulated signal set can thus be represented, during the occurrence of a pulse, by

$$f_p(t) = A \cos(p\omega_0 t), \quad (30)$$

where; p is an integer ($1 \leq p \leq N$) indicating which signal is present, A is the signal amplitude, ω_0 is the fundamental radian frequency of the signal set, and t is time. The pulse length T is an integer number of periods of the fundamental radian frequency ω_0 . Under this condition, the various demodulated signals form an orthogonal set over the pulse interval.

The optical correlator acts as a channelized, matched filter for the detection of the demodulated signals. The reference transparency thus contains N channels, each having a replica of one of the sinusoids of the demodulated set. The incoming signals are continuously recorded on the signal transparency and optically correlated with the channels of the reference.

In the optical recording processes, a time-to-space transformation

$$d = v_0 t, \quad (31)$$

is made, where d is a spatial variable, and v_0 is the recording velocity. The spatial length of a recorded signal

is thus

$$L = v_0 T. \quad (32)$$

As a function of d , a member of the signal set becomes

$$f_p(d) = A \cos\left(p \frac{w_0}{v_0} d\right). \quad (33)$$

In order to clarify the equations, the quantity $\left(\frac{w_0}{v_0}\right)$ is normalized to one. The spatial representation of a signal is then

$$f_p(d) = A \cos(pd), \quad (34)$$

during the occurrence of a pulse. These functions are optically recorded. The amplitude transmittance of the resultant signal transparency is described by $S_p(x)$, where p identifies the signal present and x represents a spatial variable (in the direction of processing) on the transparency. Similarly, the transmittance of a channel of the reference transparency is given by $R_q(y)$, where q ($1 \leq q \leq N$) denotes the channel and y is the appropriate spatial variable.

The output of channel q of the correlator with signal p present is described by

$$C_{qp}(z) = \frac{1}{L} \int_{-L/2}^{L/2} S_p(y+z) R_q(y) dy, \quad (35)$$

where L is the aperture length of the correlator (spatial equivalent of the pulse length) and $S_p(y+z)$ is the image of the recorded signal at the reference transparency plane (after displacement by the correlation variable z). The

quantity C_{qp} is the cross-correlation integral. Since L is an integer number of periods of the fundamental spatial frequency of the signal set, the various undistorted signals are orthogonal over the aperture.

In the remainder of this section, the effects of the pulsed nature of the signals on the correlation integrals are neglected. The time limitation of the signals simply imparts a triangular envelope of length $2L$ to the periodic correlation functions described here. This simplification allows the nonlinear effects to be observed without undue complication.

If the optical recording processes are linear, the amplitude transmittance of the signal transparency is described by

$$S_p(x) = a_0 + a_1 \cos(px), \quad (36)$$

where p denotes the signal present, and a_0 and a_1 are determined from the recording process used. Similarly, the transmittance of channel q of the reference transparency is

$$R_q(y) = b_0 + b_1 \cos(qy), \quad (37)$$

where b_0 and b_1 are determined by its recording process. When used in Eq. (35), the bias terms in these equations can be neglected since the correlator is assumed to contain a "d. c. stop." Substituting the resultant expressions into (35) gives

$$C_{qp}(z) = \frac{1}{L} \int_{-L/2}^{L/2} a_1 b_1 \cos[p(y+z)] \cos(qy) dy. \quad (38)$$

Evaluation yields

$$C_{qp}(z) = \begin{cases} 0, & q \neq p \\ \frac{1}{2} a, b, \cos(pz), & q = p. \end{cases} \quad (39)$$

An output thus appears in the channel of the correlator which corresponds to the input signal and indications in the others are zero. This corresponds to normal operation of the system.

When the optical recording processes are nonlinear, the signal and reference transparencies contain harmonic distortions as described in section 2.1. The resulting amplitude transmittance of the signal transparency with signal p present can be expressed by the series

$$S_p(x) = S_0 + \sum_{m=1}^{\infty} S_m \cos(mp x), \quad (40)$$

where the s harmonic coefficients result from the nonlinear characteristic of the signal recording process. In a like manner, the transmittance of channel q of the reference transparency is given by

$$R_q(y) = r_0 + \sum_{n=1}^{\infty} r_n \cos(nq y), \quad (41)$$

where the r harmonic coefficients result from the characteristic of the reference recording process. The harmonic distortions can be expressed as equivalent noise-to-signal ratios given by

$$NSR_s = \frac{\sum_{m=2}^{\infty} S_m^2}{S_1^2}, \quad (42)$$

and

$$NSR_r = \frac{\sum_{n=2}^{\infty} r_n^2}{r_1^2} \quad (43)$$

where the subscripts s and r denote, respectively, the signal and reference transparencies. The correlator can thus be considered to contain two interval equivalent noise sources.

The effects of the nonlinearities on the operation of the correlator are obtained by substitution of (40) and (41) into (35), which gives

$$C_{qp}(z) = \frac{1}{L} \int_{-L/2}^{L/2} \left\{ \sum_{m=1}^{\infty} S_m \cos[mp(y+z)] \right\} \left[\sum_{n=1}^{\infty} r_n \cos(nqy) \right] dy \quad (44)$$

when the d.c. terms are omitted. This expression can be rewritten as

$$C_{qp}(z) = \sum_{m=1}^{\infty} S_m \sum_{n=1}^{\infty} r_n \frac{1}{L} \int_{-L/2}^{L/2} \cos[mp(y+z)] \cos(nqy) dy. \quad (45)$$

Due to the orthogonality properties of the cosine functions,

$$\begin{aligned} \frac{1}{L} \int_{-L/2}^{L/2} \cos[mp(y+z)] \cos(nqy) dy \\ = \begin{cases} 0, & mp \neq nq \\ \frac{1}{2} \cos(mpz), & mp = nq, \end{cases} \end{aligned} \quad (46)$$

and Eq. (45) can be written

$$C_{qp}(z) = \frac{1}{2} \sum_{m=1}^{\infty} S_m r_m \cos(mpz) \delta_{mp, nq} \quad (47)$$

where $\delta_{mp, nq}$ is one for $mp = nq$ and zero otherwise. The output of the correlator is thus non-zero in those channels having a common frequency with the signal transparency. Outputs exist in channels corresponding to incorrect detection of the signal. The output of the correct or signal channel is

$$[C_{qp}(z)]_{p=q} = \frac{1}{2} \sum_{m=1}^{\infty} S_m r_m \cos(mpz). \quad (48)$$

Two other specific cases are:

$$[C_{qp}(z)]_{q=2p} = \frac{1}{2} \sum_{m=1}^{\infty} S_{2m} r_m \cos(2mpz), \quad (49)$$

and

$$[C_{qp}(z)]_{q=\frac{p}{2}} = \frac{1}{2} \sum_{m=1}^{\infty} S_m r_{2m} \cos(mpz). \quad (50)$$

which indicate the output of the channels corresponding to twice and half the frequency of the signal channel. Similar expressions can be obtained for other channels.

The equivalent output powers (mean squared amplitudes) of the various channels of the correlator serve as convenient measures of the severity of the nonlinear effects. Expressions for these can be obtained directly from (47) as

$$P_{qp} = \frac{1}{8} \sum_{m=1}^{\infty} S_m^2 r_m^2 \delta_{mp, nq}, \quad (51)$$

where P_{qp} indicates the equivalent output power of channel q with signal p present. This quantity can be normalized with respect to the equivalent power in the signal channel. The resulting expression

$$EPR_{qp} = \frac{P_{qp}}{[P_{qp}]_{q=p}} = \frac{\sum_{m=1}^{\infty} S_m^2 r_n^2 \delta_{mp, nq}}{\sum_{m=1}^{\infty} S_m^2 r_m^2} \quad , \quad (52)$$

indicates an "error-power ratio" existing between the outputs of channel q and the signal channel. For the signal channel, this quantity becomes unity. The definition of the EPR is similar to that of the noise-to-signal ratio introduced previously. It represents the ratio of the power of an equivalent noise source (unwanted output) to that of the desired signal.

3.2 Examples

A variety of optical recording processes can be employed to produce transparencies for use in optical correlators. The form and extent of the nonlinearities involved in these processes can vary considerably. Three examples which represent typically occurring nonlinearities are considered. In each example, it is assumed that a single characteristic describes both the signal and reference recording processes. The harmonic series of the resultant transparency for each characteristic are derived and the

corresponding NSR's and EPR's calculated.

The characteristic for the first example is linear. That of the second follows a square law and that of the third an exponential. A linear characteristic can result from use of a small operating region within a larger nonlinear characteristic or from using pre-distortion techniques to cancel nonlinear effects. Characteristics approaching square law and exponential curves can be obtained, respectively, from positive and negative photographic processes used in conjunction with primary light modulators such as cathode ray tubes.

The characteristics for the optical recording processes of the three examples are shown in Figures 2 through 4. They describe the variation of the amplitude transmittance of a resulting transparency with input voltage. In the examples, the signals are assumed to be recorded with a bias level of .5v and an amplitude of .3v. The spatial representations of the electrical inputs are thus

$$V_p(d) = .5 + .3 \cos(pd). \quad (53)$$

In the linear case, the amplitude transmittance of the signal transparency with signal P present becomes

$$S_p(x) = .5 + .3 \cos(px), \quad (54)$$

and the transmittance of channel q of the reference is

$$R_q(y) = .5 + .3 \cos(qy). \quad (55)$$

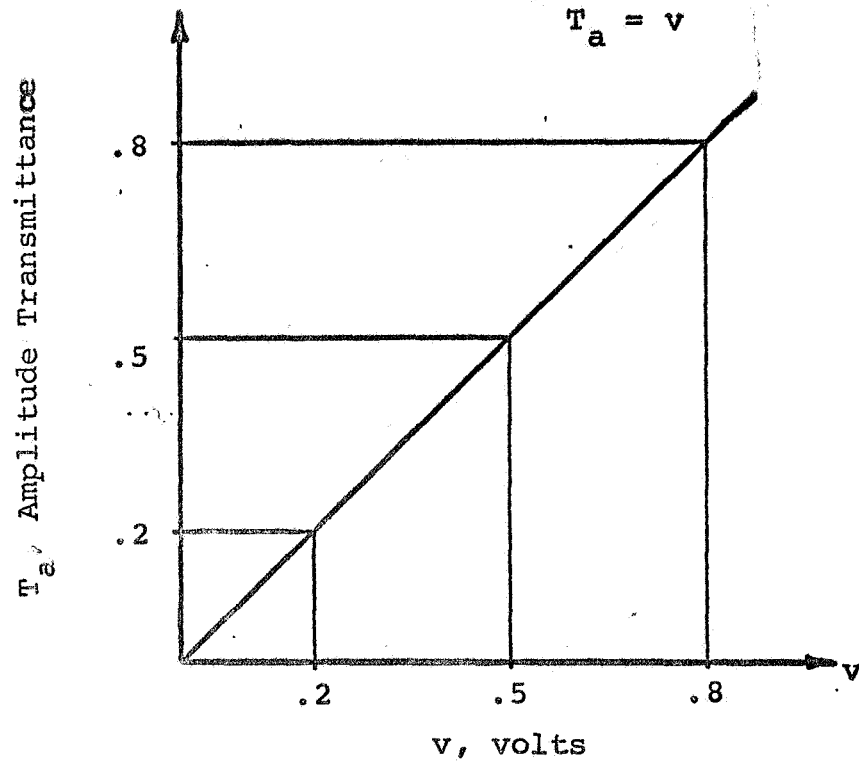


Figure 2. A linear characteristic

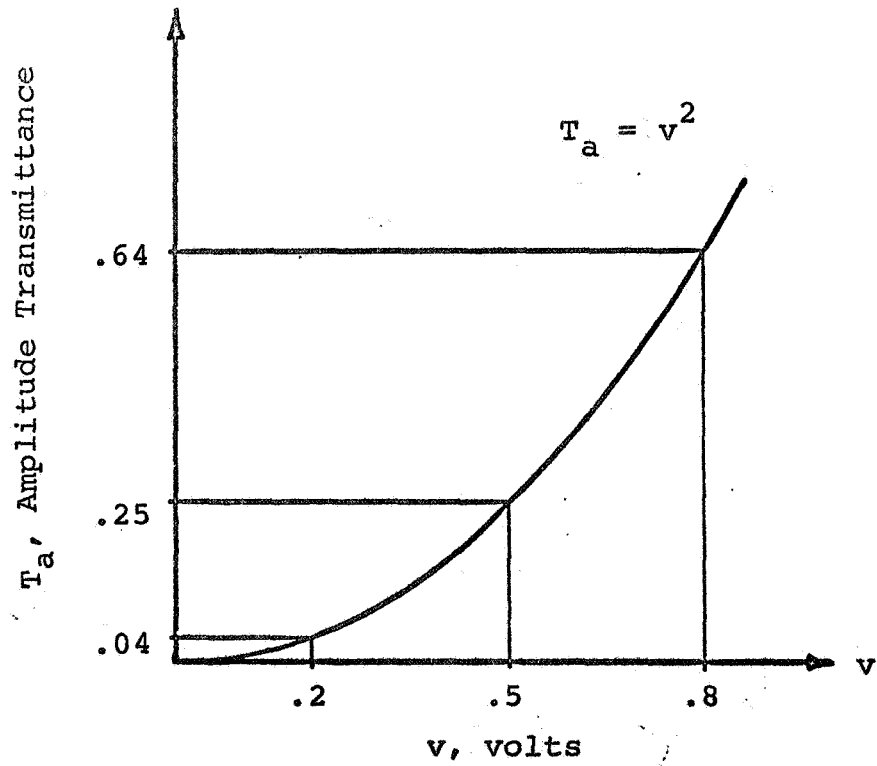


Figure 3. A square law characteristic

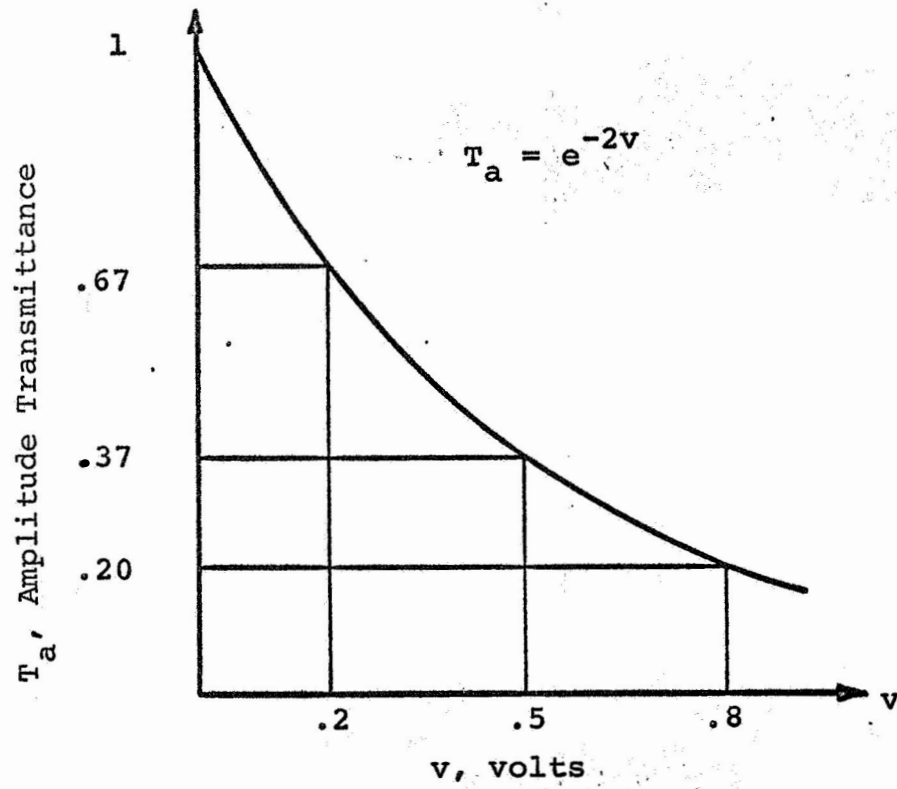


Figure 4. An exponential characteristic

Since no distortions are present, the corresponding noise-to-signal ratios are zero. With signal p present, the correlator output in the signal channel is

$$[C_{qp}(z)]_{p=q} = (.045) \cos(pz). \quad (56)$$

Outputs of the other channels are zero and the corresponding error-power ratios vanish as shown in Table 1. The correlator thus operates normally.

In the square law example, the amplitude transmittance of the transparencies are described by

$$S_p(x) = [.5 + .3 \cos(px)]^2,$$

and

$$R_q(y) = [.5 + .3 \cos(qy)]^2,$$

or, after expanding

$$S_p(x) = (.295) + (.3) \cos(px) + (.045) \cos(2px), \quad (57)$$

and

$$R_q(y) = (.295) + (.3) \cos(qy) + (.045) \cos(2qy). \quad (58)$$

The signal transparency and reference channels thus contain second harmonic distortions. The corresponding noise-to-signal ratios are

$$NSR_s = .225 \times 10^{-1}, \quad (59)$$

and

$$NSR_r = .225 \times 10^{-1}. \quad (60)$$

Because of the harmonics, unwanted outputs occur in channels corresponding to twice and half the frequency of the signal channel. The resulting error-power ratios, calculated from

Table 1. Error-power ratios corresponding to three optical recording characteristics

Signal-Reference Channel Relation q/p	Characteristic		
	Linear	Square Law	Exponential
1	1.0	1.0	1.0
1/2, 2	0	$.2249 \times 10^{-1}$	$.2184 \times 10^{-1}$
1/3, 3	0	0	$.2045 \times 10^{-3}$
1/4, 4	0	0	$.1690 \times 10^{-5}$
2/3, 3/2	0	0	$.4471 \times 10^{-5}$
3/4, 4/3	0	0	$.3458 \times 10^{-9}$

the harmonic coefficients of (57) and (58), and the definition (52) are shown in Table 1.

In the exponential case, the form of the recorded signal can be obtained from a Taylor series expansion of the characteristic about the bias point. Neglecting orders higher than the fourth, the amplitude transmittance is given by

$$T_a(v) = \frac{1}{e} \left[1 - 2(v-.5) + 2(v-.5)^2 - \frac{4}{3}(v-.5)^3 + \frac{2}{3}(v-.5)^4 \right]. \quad (61)$$

Substituting (53) in this expression and expanding the resulting powers of the cosine function into multiple angles gives

$$S_p(x) = (.4017) - (.2307) \cos(px) + (.0341) \cos(2px) \\ - (.0033) \cos(3px) + (.0003) \cos(4px), \quad (62)$$

for the signal transparency and a similar expression for the reference channels $R_q(Y)$. The noise-to-signal ratios corresponding to these expressions are

$$NSR_s = .2206 \times 10^{-1}, \quad (63)$$

and

$$NSR_r = .2206 \times 10^{-1}. \quad (64)$$

Harmonics higher than the fourth do not appear in the expression (62) due to the truncation of the Taylor series. The higher order terms of this series give rise to additional harmonics and small contributions to the ones retained above. These are neglected here. The four harmonics of Eq. (62) give rise to outputs in the channels listed in Table 1. The

error-power ratios shown were calculated from the coefficients of (62) and the definition (52).

In this example, the Taylor series expansion was employed to obtain the harmonic coefficients of the recorded signals. Versions of this method have been used by several authors as described in the summary of the literature. Other series expansions may be used, however. The Taylor method and some of these are described more thoroughly in the next section.

4. EXPANSION METHODS FOR DETERMINING HARMONIC COEFFICIENTS

4.1 Introduction

The harmonic coefficients of the output of a sinusoidally excited (zero-memory) nonlinear device may be obtained by expanding, within the operating region, the characteristic function of the device. Equations can be developed relating the expansion coefficients of the characteristic to the output coefficients. The Tchebyscheff (Tischer, 1967), Legendre, Fourier, and Taylor expansions are among those suitable for this purpose. Equations relating the output harmonic coefficients to the expansion coefficients of these series are derived in this section. Relative advantages of the various methods are also discussed.

Two versions of the Fourier series method are presented. In method A, a direct expansion of the nonlinear characteristic is performed within the operating region. This method has a disadvantage in that if the characteristic is continuous within this region ($[a,b]$), but does not meet the boundary condition

$$f(a) = f(b), \quad (65)$$

its periodic extension is discontinuous. The resulting Fourier series is slowly convergent (Lanczos, 1966). This problem can be avoided, provided $f(x)$ is continuous on $[a,b]$, by extending the characteristic symmetrically about either of the end points. The periodic extension of the resulting function is continuous and its Fourier series more quickly

convergent (Lanczos, 1966). This series can then be used to represent the characteristic function within the operating region. This procedure is employed in method B. More sophisticated schemes, not considered here, can be used to further increase the rate of convergence of the Fourier series provided successively higher derivatives of $f(x)$ are continuous (Lanczos, 1966).

In order to clarify the equations of this section, the following notation is adopted. The nonlinear characteristic is termed $f(x)$. The operating region is assumed to be $[-1,1]$ and the input sinusoid given by

$$x = \cos \theta. \quad (66)$$

The output of the nonlinear device is then $f(\cos \theta)$. Since this is an even function in θ , its Fourier series expansion has the form

$$f(\cos \theta) = \frac{1}{2} \sum_{k=0}^{\infty} \epsilon_k b_k \cos(k\theta), \quad (67)$$

where

$$b_k = \frac{2}{\pi} \int_0^{\pi} f(\cos \theta) \cos(k\theta) d\theta, \quad (68)$$

and the Neumann symbol ϵ_k is given by

$$\epsilon_0 = 1, \quad (69)$$

$$\epsilon_1 = \epsilon_2 = \dots = 2. \quad (70)$$

The definition of the symbol is used throughout this chapter.

In the derivations which follow, the orders of integra-

tion and summation of infinite series of functions are interchanged at various times. This procedure is justified by Arzelà's theorem (Apostol, 1957).

4.2 Taylor Series

The Taylor series expansion, about $x = 0$, of $f(x)$ on $[-1,1]$ is given by

$$f(x) = \sum_{n=0}^{\infty} a_n x^n \quad (71)$$

where

$$a_n = \frac{1}{n!} \left[\frac{d^n}{dx^n} f(x) \right]_{x=0} \quad (72)$$

If $f(x)$ and its derivatives are continuous on an interval containing $[-1,1]$, the series converges (Kaplan, 1952). Replacing x by $\cos \theta$ in Eq. (71) gives

$$f(\cos \theta) = \sum_{n=0}^{\infty} a_n (\cos \theta)^n, \quad (73)$$

which may be substituted into the Eq. (68) for the k^{th} output harmonic coefficient yielding

$$b_k = \frac{2}{\pi} \int_0^{\pi} \left[\sum_{n=0}^{\infty} a_n (\cos \theta)^n \right] \cos(k\theta) d\theta. \quad (74)$$

The order of integration and summation may be interchanged in this expression so that

$$b_k = \frac{2}{\pi} \sum_{n=0}^{\infty} a_n \int_0^{\pi} (\cos \theta)^n \cos(k\theta) d\theta. \quad (75)$$

The integrals in this expression can be evaluated using the expansion (Mangulis, 1965)

$$(\cos \theta)^n = \left(\frac{1}{2}\right)^n \sum_{m=0,2,\dots}^n \epsilon_m \binom{n}{\frac{n-m}{2}} \cos(m\theta), \quad (76)$$

for even n and

$$(\cos \theta)^n = \left(\frac{1}{2}\right)^{n-1} \sum_{m=1,3,\dots}^n \binom{n}{\frac{n-m}{2}} \cos(m\theta), \quad (77)$$

for odd n where the large brackets denote binomial coefficients. Substituting these into the integrals of (75) and interchanging the orders of integration and summation gives

$$\begin{aligned} \int_0^\pi (\cos \theta)^n \cos(k\theta) d\theta &= \\ \left(\frac{1}{2}\right)^n \sum_{m=0,2,\dots}^n \epsilon_m \binom{n}{\frac{n-m}{2}} \int_0^\pi \cos(m\theta) \cos(k\theta) d\theta, \end{aligned} \quad (78)$$

for even n and

$$\begin{aligned} \int_0^\pi (\cos \theta)^n \cos(k\theta) d\theta &= \\ \left(\frac{1}{2}\right)^{n-1} \sum_{m=1,3,\dots}^n \binom{n}{\frac{n-m}{2}} \int_0^\pi \cos(m\theta) \cos(k\theta) d\theta, \end{aligned} \quad (79)$$

for odd n . Evaluation of the remaining integrals gives

$$\int_0^\pi (\cos \theta)^n \cos(k\theta) d\theta = \begin{cases} 0, & n < k \\ \frac{\pi}{2} \left(\frac{1}{2}\right)^{n-1} \binom{n}{\frac{n-k}{2}}, & n \geq k, \end{cases} \quad (80)$$

for all n . Equation (75) thus becomes

$$b_k = \sum_{n=k, k+2, \dots}^{\infty} a_n \left(\frac{1}{2}\right)^{n-1} \binom{n}{\frac{n-k}{2}}. \quad (81)$$

This expresses the output harmonic coefficients b_k in terms of the Taylor coefficients a_n .

4.3 Fourier Series - Method A

The direct Fourier series expansion of $f(x)$ on $[-1,1]$ can be written as

$$f(x) = \frac{1}{2} \sum_{n=0}^{\infty} e_n [c_n \cos(n\pi x) + d_n \sin(n\pi x)], \quad (82)$$

where

$$c_n = \int_{-1}^1 f(x) \cos(n\pi x) dx, \quad (83)$$

and

$$d_n = \int_{-1}^1 f(x) \sin(n\pi x) dx. \quad (84)$$

A sufficient condition for the pointwise convergence of this expansion on $[-1,1]$ is that $f(x)$ is sectionally continuous and square integrable on $[-1,1]$ (Jackson, 1941). Replacing x by $\cos \theta$ in Eq. (82) gives

$$f(\cos \theta) = \frac{1}{2} \sum_{n=0}^{\infty} e_n [c_n \cos(n\pi \cos \theta) + d_n \sin(n\pi \cos \theta)] \quad (85)$$

which is pointwise convergent for $0 \leq \theta \leq \pi$. The equation giving

the k^{th} output harmonic coefficient is

$$b_k = \frac{2}{\pi} \sum_{n \neq 0}^{\infty} \int_0^{\pi} f(\cos \theta) \cos(k\theta) d\theta. \quad (86)$$

Substituting the series of Eq. (85) and interchanging the orders of integration and summation gives

$$b_k = \frac{1}{\pi} \sum_{n=0}^{\infty} \epsilon_n \left[c_n \int_0^{\pi} \cos(n\pi \cos \theta) \cos(k\theta) d\theta + d_n \int_0^{\pi} \sin(n\pi \cos \theta) \cos(k\theta) d\theta \right]. \quad (87)$$

The integrals here may be evaluated by using the expansions (Mangulis, 1965)

$$\cos(n\pi \cos \theta) = \sum_{l=0,2,\dots}^{\infty} \epsilon_l (-1)^{l/2} J_l(n\pi) \cos(l\theta) \quad (88)$$

and

$$\sin(n\pi \cos \theta) = 2 \sum_{l=1,3,\dots}^{\infty} (-1)^{(l-1)/2} J_l(n\pi) \cos(l\theta), \quad (89)$$

where J_l is the l^{th} order Bessel function of the first type. Substituting these into the integrals of Eq. (87), and again interchanging orders of integration and summation gives

$$\int_0^{\pi} \cos(n\pi \cos \theta) \cos(k\theta) d\theta = \sum_{l=0,2}^{\infty} \epsilon_l (-1)^{l/2} J_l(n\pi) \int_0^{\pi} \cos(l\theta) \cos(k\theta) d\theta, \quad (90)$$

and

$$\int_0^\pi \sin(n\pi \cos \theta) \cos(k\theta) d\theta = 2 \sum_{l=1,3,\dots}^{\infty} (-1)^{\frac{l-1}{2}} J_l(n\pi) \int_0^\pi \cos(l\theta) \cos(k\theta) d\theta. \quad (91)$$

Evaluation yields

$$\int_0^\pi \cos(n\pi \cos \theta) \cos(k\theta) d\theta = \begin{cases} 0, & k \text{ odd} \\ (-1)^{k/2} \pi J_k(n\pi), & k \text{ even} \end{cases}, \quad (92)$$

and

$$\int_0^\pi \sin(n\pi \cos \theta) \cos(k\theta) d\theta = \begin{cases} (-1)^{\frac{k-1}{2}} \pi J_k(n\pi), & k \text{ odd} \\ 0, & k \text{ even} \end{cases}. \quad (93)$$

Substituting these results into (87) gives

$$b_k = (-1)^{k/2} \sum_{n=0}^{\infty} \epsilon_n c_n J_k(n\pi), \quad (94)$$

for even k and

$$b_k = 2(-1)^{\frac{k-1}{2}} \sum_{n=0}^{\infty} d_n J_k(n\pi), \quad (95)$$

for odd k . These are the resulting expressions for the output harmonic coefficients.

4.4 Fourier Series - Method B

A Fourier series expression for $f(x)$ on $[-1,1]$ may be obtained by defining a related function $g(x)$ on $[-2,2]$. On $[0,2]$, $g(x)$ is the translation of $f(x)$ given by

$$g(x) = f(x - 1). \quad (96)$$

On $[-2,0]$, $g(x)$ is extended evenly. Because of the evenness property, the Fourier series expansion of $g(x)$ on $[-2,2]$ contains only cosine terms. This expansion is then given by

$$g(x) = \frac{1}{2} \sum_{n=0}^{\infty} \epsilon_n a_n \cos\left(\frac{n\pi}{2} x\right), \quad (97)$$

where

$$a_n = \int_0^2 g(x) \cos\left(\frac{n\pi}{2} x\right) dx. \quad (98)$$

The coefficients a_n can also be evaluated in terms of $f(x)$ as

$$a_n = \int_{-1}^1 f(x) \cos\left[\frac{n\pi}{2}(x+1)\right] dx. \quad (99)$$

Replacing x by $x + 1$ in Eq. (97) and using Eq. (96) gives

$$f(x) = \frac{1}{2} \sum_{n=0}^{\infty} \epsilon_n a_n \cos\left[\frac{n\pi}{2}(x+1)\right] \quad (100)$$

or

$$f(x) = \frac{1}{2} \sum_{n=0}^{\infty} \epsilon_n a_n \left[\cos\left(\frac{n\pi}{2}\right) \cos\left(\frac{n\pi}{2} x\right) - \sin\left(\frac{n\pi}{2}\right) \sin\left(\frac{n\pi}{2} x\right) \right] \quad (101)$$

Substituting $\cos \theta$ for x in this expression and using the resulting series in the equation for the k^{th} output Fourier

coefficient gives

$$b_k = \frac{1}{\pi} \int_0^{\pi} \left\{ \sum_{n=0}^{\infty} \epsilon_n a_n \left[\cos\left(\frac{n\pi}{2}\right) \cos\left(\frac{n\pi}{2} \cos\theta\right) - \sin\left(\frac{n\pi}{2}\right) \sin\left(\frac{n\pi}{2} \cos\theta\right) \right] \right\} \cos(k\theta) d\theta. \quad (102)$$

Interchanging the order of integration and summation yields

$$b_k = \frac{1}{\pi} \sum_{n=0}^{\infty} \epsilon_n a_n \left[\cos\left(\frac{n\pi}{2}\right) \int_0^{\pi} \cos\left(\frac{n\pi}{2} \cos\theta\right) \cos(k\theta) d\theta - \sin\left(\frac{n\pi}{2}\right) \int_0^{\pi} \sin\left(\frac{n\pi}{2} \cos\theta\right) \cos(k\theta) d\theta \right]. \quad (103)$$

The integrals in this expression may be evaluated using the expansions (88) and (89) where $n\pi$ is replaced by $\frac{n\pi}{2}$. Using these as in the previous derivation gives

$$\int_0^{\pi} \cos\left(\frac{n\pi}{2} \cos\theta\right) \cos(k\theta) d\theta = \begin{cases} (-1)^{k/2} \pi J_k\left(\frac{n\pi}{2}\right), & k \text{ even} \\ 0, & k \text{ odd} \end{cases} \quad (104)$$

and

$$\int_0^{\pi} \sin\left(\frac{n\pi}{2} \cos\theta\right) \cos(k\theta) d\theta = \begin{cases} 0, & k \text{ even} \\ (-1)^{\frac{k-1}{2}} \pi J_k\left(\frac{n\pi}{2}\right), & k \text{ odd.} \end{cases} \quad (105)$$

Substituting these results in (103) gives the equations for the output harmonic coefficients:

$$b_k = (-1)^{k/2} \sum_{n=0,2,\dots}^{\infty} \epsilon_n a_n (-1)^{n/2} J_k\left(\frac{n\pi}{2}\right), \quad (106)$$

for even k and

$$b_k = 2(-1)^{\frac{k-1}{2}} \sum_{n=1,3,\dots}^{\infty} a_n (-1)^{\frac{n-1}{2}} J_k\left(\frac{n\pi}{2}\right), \quad (107)$$

for odd k .

4.5 Legendre Series

The Legendre series expansion (Kaplan, 1952) of $f(x)$ on $[-1,1]$ is given by

$$f(x) = \sum_{n=0}^{\infty} a_n P_n(x), \quad (108)$$

where

$$a_n = \frac{2n+1}{2} \int_{-1}^1 f(x) P_n(x) dx, \quad (109)$$

and P_n is the Legendre polynomial of order n . A sufficient condition for the pointwise convergence of the series (106) on $[-1,1]$ is that $f(x)$ is sectionally continuous and square integrable on $[-1,1]$ (Jackson, 1941). The Legendre polynomials can be defined by

$$P_0(x) = 1, \quad (110)$$

$$P_1(x) = x, \quad (111)$$

and the recurrence relation

$$P_{n+1}(x) = \frac{2n+1}{n+1} x P_n(x) - \frac{n}{n+1} P_{n-1}(x), \quad (112)$$

or by Rodrigues' formula

$$P_n(x) = \frac{1}{2^n n!} \frac{d^n}{dx^n} [(x^2-1)^n] \quad (113)$$

Replacing x by $\cos \theta$ in Eq. (108) gives

$$f(\cos \theta) = \sum_{n=0}^{\infty} a_n P_n(\cos \theta). \quad (114)$$

The pointwise convergence of (106) on $[-1,1]$ implies the pointwise convergence of this expression for $0 < \theta < \pi$. Equation (112) may be substituted into the equation for the k^{th} output harmonic coefficient,

$$b_k = \frac{2}{\pi} \int_0^{\pi} f(\cos \theta) \cos(k\theta) d\theta, \quad (115)$$

giving

$$b_k = \frac{2}{\pi} \int_0^{\pi} \left[\sum_{n=0}^{\infty} a_n P_n(\cos \theta) \right] \cos(k\theta) d\theta. \quad (116)$$

Since the series (114) is pointwise convergent on $(0, \pi)$, the order of integration and summation in this expression can be interchanged so that

$$b_k = \frac{2}{\pi} \sum_{n=0}^{\infty} a_n \left[\int_0^{\pi} P_n(\cos \theta) \cos(k\theta) d\theta \right]. \quad (117)$$

The integrals in this expression can be evaluated using the expansions (Mangulis, 1965)

$$P_n(\cos \theta) = \frac{1}{\pi} \sum_{l=0,2,\dots}^n \epsilon_l \frac{\Gamma(\frac{n-l+1}{2}) \Gamma(\frac{n+l+1}{2})}{(\frac{n-l}{2})! (\frac{n+l}{2})!} \cos(l\theta), \quad (118)$$

for even n and

$$P_n(\cos \theta) = \frac{2}{\pi} \sum_{l=1,3,\dots}^n \frac{\Gamma(\frac{n-l+1}{2}) \Gamma(\frac{n+l+1}{2})}{(\frac{n-l}{2})! (\frac{n+l}{2})!} \cos(l\theta), \quad (119)$$

for odd n , where Γ represents the gamma function. Substituting these expansions in the integrals and again inter-

changing orders of integration and summation gives

$$\int_0^\pi P_n(\cos\theta) \cos(k\theta) d\theta = \frac{1}{\pi} \sum_{l=0,2,\dots}^n a_l \frac{\Gamma(\frac{n-l+1}{2}) \Gamma(\frac{n+l+1}{2})}{(\frac{n-l}{2})! (\frac{n+l}{2})!} \int_0^\pi \cos(l\theta) \cos(k\theta) d\theta, \quad (120)$$

for even n and

$$\int_0^\pi P_n(\cos\theta) \cos(k\theta) d\theta = \frac{2}{\pi} \sum_{l=1,3,\dots}^n \frac{\Gamma(\frac{n-l+1}{2}) \Gamma(\frac{n+l+1}{2})}{(\frac{n-l}{2})! (\frac{n+l}{2})!} \int_0^\pi \cos(l\theta) \cos(k\theta) d\theta, \quad (121)$$

for odd n . Evaluating the integrals in these expressions gives

$$\int_0^\pi P_n(\cos\theta) \cos(k\theta) d\theta = \begin{cases} 0, & n < k \\ \frac{\Gamma(\frac{n-k+1}{2}) \Gamma(\frac{n+k+1}{2})}{(\frac{n-k}{2})! (\frac{n+k}{2})!}, & n \geq k \end{cases}, \quad (122)$$

for both even and odd n . Substitution of this result in (117) yields

$$b_k = \frac{2}{\pi} \sum_{n=k, k+2, \dots}^{\infty} a_n \frac{\Gamma(\frac{n-k+1}{2}) \Gamma(\frac{n+k+1}{2})}{(\frac{n-k}{2})! (\frac{n+k}{2})!}. \quad (123)$$

This expression, then, gives the output harmonic coefficients b_k in terms of the Legendre expansion coefficients.

4.6 Tchebyscheff Series

The Tchebyscheff expansion (Snyder, 1966) of a function $f(x)$ on the interval $[-1,1]$ is given by

$$f(x) = \frac{1}{2} \sum_{n=0}^{\infty} \epsilon_n a_n T_n(x) \quad (124)$$

and

$$a_n = \frac{2}{\pi} \int_{-1}^1 \frac{f(x) T_n(x)}{\sqrt{1-x^2}} dx, \quad (125)$$

where $T_n(x)$ represents the Tchebyscheff polynomial of order n . A sufficient condition for the convergence of (124) is that $f(x)$ is piecewise continuous on $[-1,1]$. The Tchebyscheff polynomials can be defined by

$$T_0(x) = 1,$$

$$T_1(x) = x,$$

and the recurrence relation

$$T_{n+1}(x) = 2x T_n(x) - T_{n-1}(x), \quad (126)$$

or the "Rodrigues" formula

$$T_n(x) = \frac{(-1)^n 2^n n!}{(2n)!} (1-x^2)^{1/2} \frac{d^n}{dx^n} \left[(1-x^2)^{\frac{n-2}{2}} \right]. \quad (127)$$

The polynomials can be alternately expressed as

$$T_n(x) = \cos(n \cos^{-1} x). \quad (128)$$

When $\cos \theta$ is substituted for x ,

$$T_n(\cos \theta) = \cos(n\theta). \quad (129)$$

Equation (124) then can be written as

$$f(\cos \theta) = \frac{1}{2} \sum_{n=0}^{\infty} \epsilon_n a_n \cos(n\theta), \quad (130)$$

and Eq. (123) as

$$a_n = \frac{2}{\pi} \int_0^{\pi} f(\cos \theta) \cos(n\theta) d\theta. \quad (131)$$

These equations are recognized as those of Fourier expansion of the output of the nonlinear device. The various Tchebyscheff polynomials which form the expansion of $f(x)$ thus correspond to the harmonics of the output signal. The harmonic coefficients b_k of Eq. (68) are then given simply by

$$b_k = a_k \quad (132)$$

Because of this unique property of the Tchebyscheff polynomials, the harmonic coefficients of the output of the nonlinear device can be obtained directly from the expansion of its characteristic. The other expansion methods described do not have this property. It should be noted, however, that the equivalence of the Tchebyscheff and harmonic coefficients exists only when the change of variable $x = \cos \theta$ is made. When the amplitude of the cosine is other than one, the right-hand side of Eq. (129) is replaced by a series expression. The resulting equations for the b_k involve infinite sums. This difficulty can be overcome in the general case by appropriate normalization of the expansion interval.

4.7 Relative Advantages

All of the preceding expansion methods can be used to determine the effects of nonlinearities on sinusoidal signals. The harmonic coefficients of the output are given, in terms of the various expansion coefficients, by the relations derived.

The Tchebyscheff expansion method has significant advantages in that its coefficients are equal to those of the output harmonics. The summations required by the other methods are avoided. This is of value since the sums must be truncated in most applications. The truncation introduces errors into the expressions for the output harmonic coefficients and convergence must be considered.

Use of any of the methods requires the expansion coefficients to be obtained from the nonlinear characteristic. The advantages of any one of the methods, in this respect, are not readily apparent. The ease of calculation of the various sets of coefficients depends on the form of the given characteristic. In specific cases, any one set may be most easily evaluated.

5. COMPARISON OF THE EXPANSION METHODS

This section presents a comparison of the use of the various expansion methods for obtaining the harmonic coefficients of the output of a nonlinear device. Approximations to the coefficients are obtained from truncated Legendre, Fourier, and Taylor expansions of orders two through nine. These approximations are compared with values given by the Tchebyscheff method. Output harmonics of orders one through four are considered.

Computer programs were used to obtain the Tchebyscheff (RCH), Legendre (LEG), Fourier (FOU), and modified Fourier (FOB), and Taylor (LMS) expansion coefficients for the characteristic shown in Figure 5. This curve is typical of high-gamma photographic processes used in optical data processing and holography. Except for the Taylor series method, numerical integration procedures were used to obtain the expansion coefficients. The Taylor series coefficients were obtained by the least-squares method of curve fitting. The Tchebyscheff coefficients were obtained using the method described in the following section.

The expansion coefficients were then used in the expressions derived in section 5 for the output harmonic coefficients. The results for harmonic coefficients of order one through four given by truncating the expansions at orders two through nine are shown in Figures 6 through 9. The trend of convergence to the Tchebyscheff values as

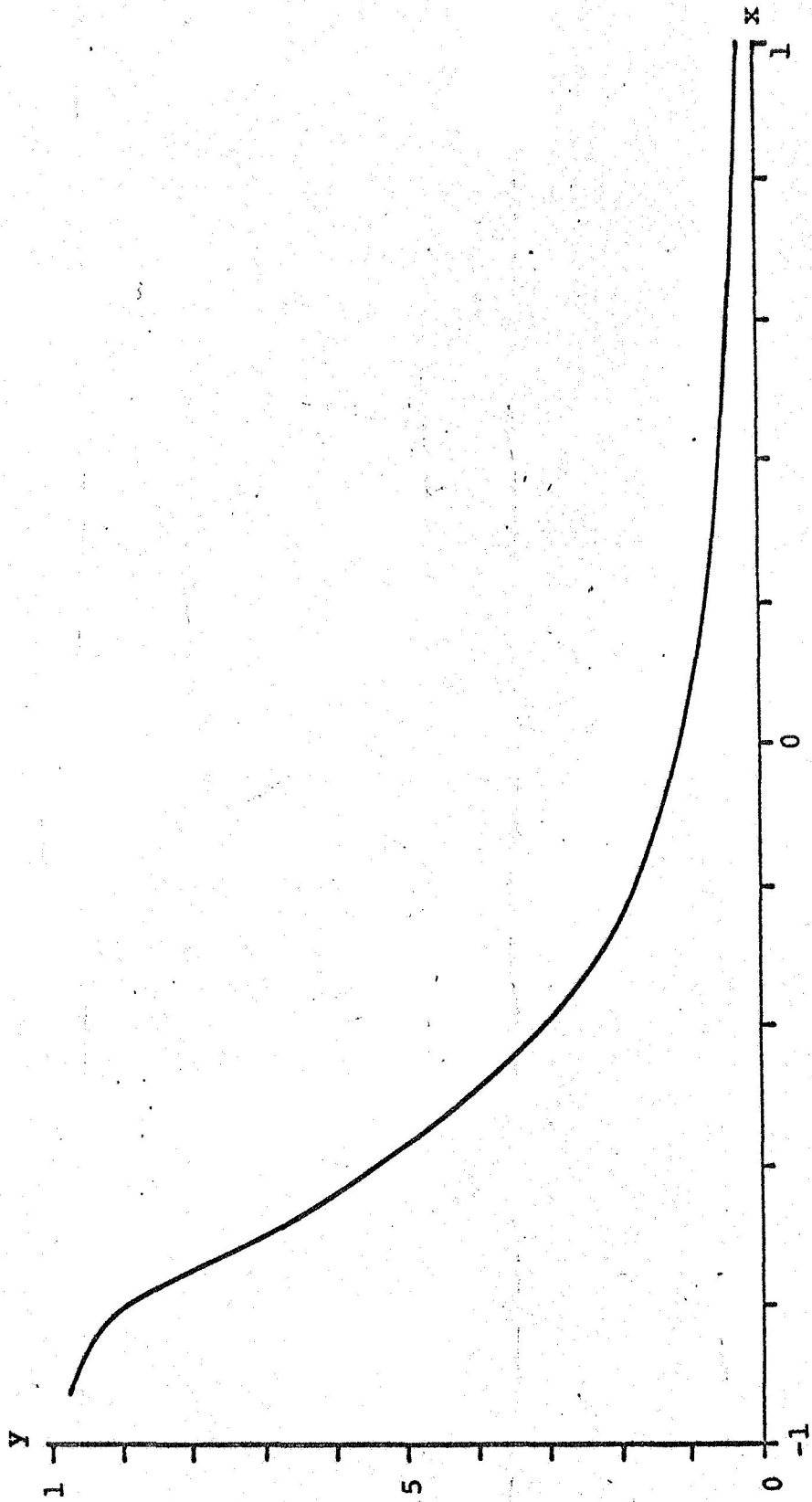


Figure 5. Typical "high-gamma" characteristic normalized to [-1,1]

the expansion order is increased can be seen.

The figures demonstrate the advantages of using the Tchebyscheff expansion method. The TCH values are given directly by the first four expansion coefficients. Higher order terms are unnecessary. The convergence of the approximations given by the other methods varies somewhat with the output harmonic order. In most instances, at least sixth order expansions were necessary for good convergence. The improved convergence of the FOB method is apparent.

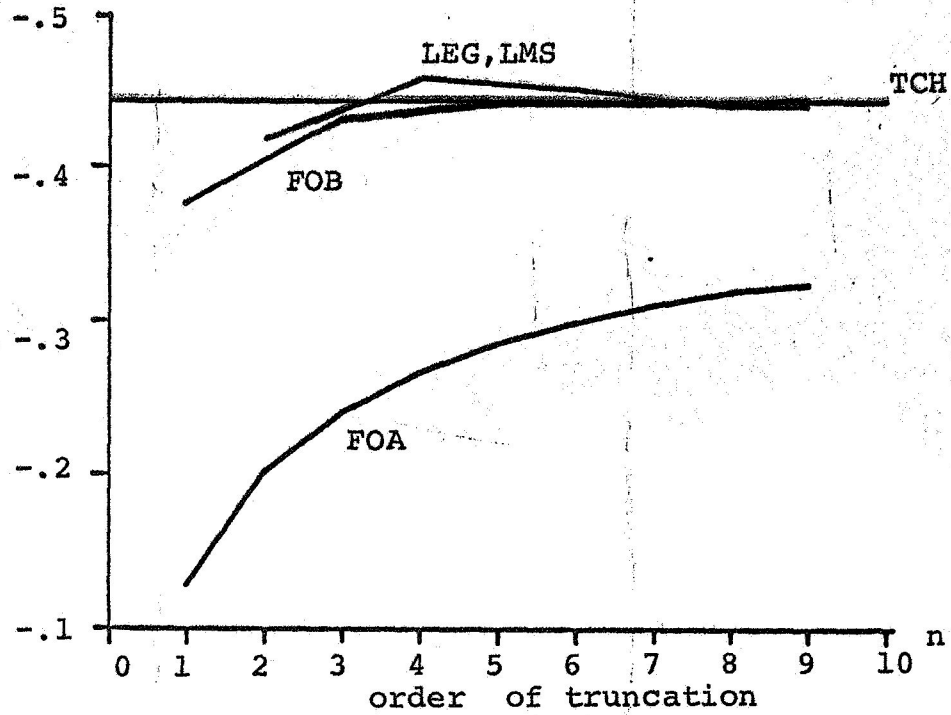


Figure 6. Approximations to the harmonic coefficient b_1

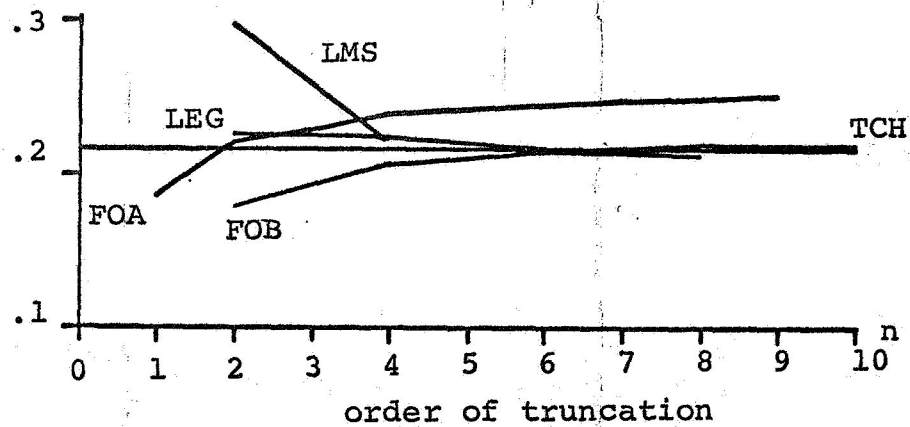


Figure 7. Approximations to the harmonic coefficient b_2

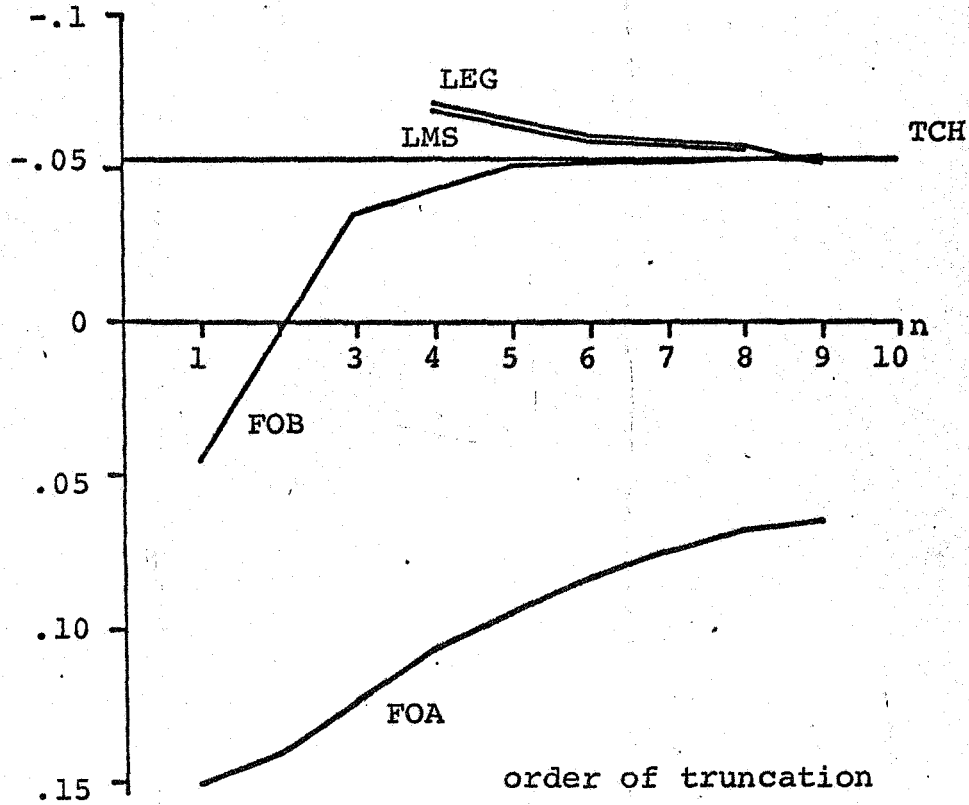


Figure 8. Approximations to the harmonic coefficient b_3

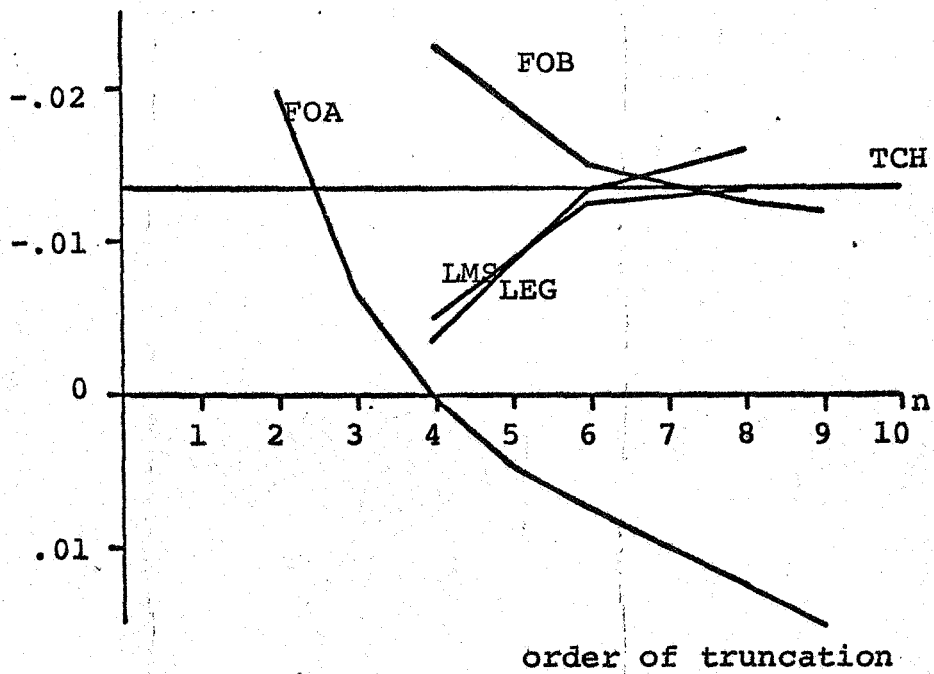


Figure 9. Approximations to the harmonic coefficient b_4

6. A NUMERICAL METHOD FOR COMPUTING TCHEBYSCHIEFF COEFFICIENTS

Previous sections demonstrate the advantages of using the Tchebyscheff expansion method for determining the output harmonic coefficients of a nonlinear device. The application of this method to actual problems necessitates the determination of the Tchebyscheff coefficients from the characteristic functions. This section describes a numerical method to accomplish this.

In the study of nonlinear devices, the characteristic function (or transfer characteristic) may be given either analytically, graphically, or numerically. The method presented here can be used with characteristics given in any of these forms. It consists of representing the characteristic by a piecewise linear approximation and then calculating analytically the Tchebyscheff coefficients of this representation. Since the only approximations introduced are those in the piecewise representation of the characteristic, this method seems to have advantages over the direct application of numerical integration.

Figure 10 shows a typical nonlinear characteristic $f(x)$ and a region where the Tchebyscheff expansion is desired. The region is given by

$$|x - x_0| \leq A. \quad (133)$$

Making the change of variable

$$u = \frac{x - x_0}{A}, \quad (134)$$

the region in u is

$$|u| \leq 1. \quad (135)$$

The expansion coefficients are then given by either

$$a_n(A, x_0) = \frac{2}{\pi} \int_{-1}^1 \frac{f(Au + x_0) T_n(u)}{\sqrt{1-u^2}} du, \quad (136)$$

or

$$a_n(A, x_0) = \frac{2}{\pi} \int_0^\pi f(A \cos \theta + x_0) \cos(n\theta) d\theta, \quad (137)$$

as was shown previously. These equations can be simplified by defining

$$g(u) = f(Au + x_0), \quad (138)$$

in the region given by (135). Equations (136) and (137) then become

$$a_n(A, x_0) = \frac{2}{\pi} \int_{-1}^1 \frac{g(u) T_n(u)}{\sqrt{1-u^2}} du, \quad (139)$$

and

$$a_n(A, x_0) = \frac{2}{\pi} \int_0^\pi g(\cos \theta) \cos(n\theta) d\theta. \quad (140)$$

The function $g(u)$ can be represented by a piecewise linear approximation consisting of N segments as shown in Figure 11. When $g(u)$ is continuous, the error in the approximation can be made arbitrarily small by increasing the number of segments N such that the length of each becomes small. If a set of $N + 1$ values of u and $g(u)$ including the endpoints of the interval $|u| \leq 1$ are known, the equations

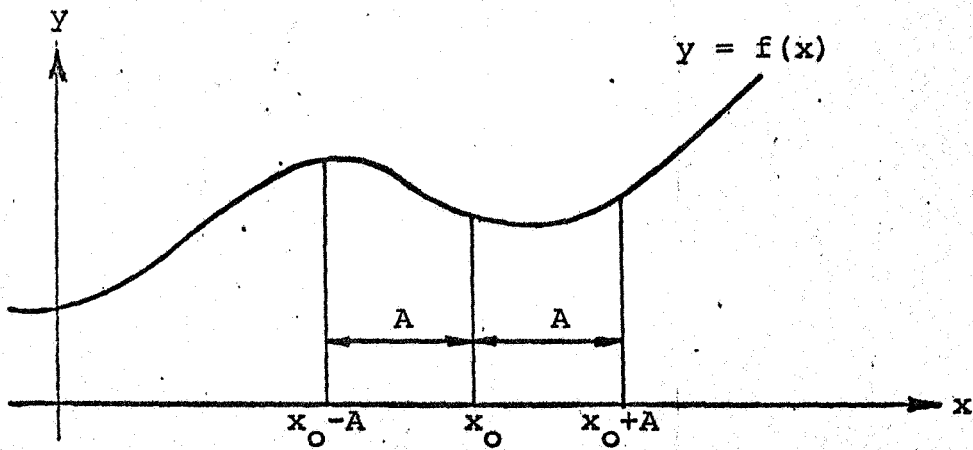


Figure 10. Typical characteristic and desired expansion region

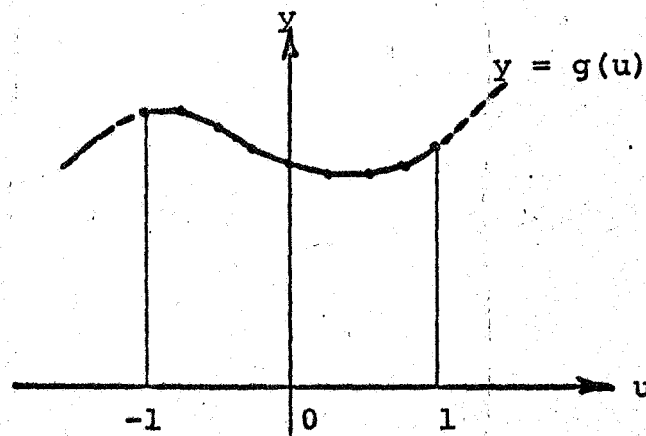


Figure 11. A piecewise linear approximation to the characteristic

of the corresponding segments can be computed. Denoting the values of u and g by u_i and $g(u_i)$, where $1 \leq i \leq N+1$, the Tchebyscheff expansion coefficients for the approximation to $g(u)$ are given by

$$Q_n = \frac{2}{\pi} \sum_{i=1}^N \int_{u_i}^{u_{i+1}} \frac{(c_i + d_i u) T_n(u)}{\sqrt{1-u^2}} du, \quad (141)$$

where $(c_i$ and $d_i u)$ represents the equation for the i^{th} segment. The constants c_i and d_i can be computed by solving the equations

$$c_i + d_i u_i = g(u_i), \quad (142)$$

and

$$c_i + d_i u_{i+1} = g(u_{i+1}), \quad (143)$$

which give

$$c_i = \frac{g(u_i) u_{i+1} - g(u_{i+1}) u_i}{u_{i+1} - u_i}, \quad (144)$$

and

$$d_i = \frac{g(u_{i+1}) - g(u_i)}{u_{i+1} - u_i}, \quad (145)$$

Equation (139) can be evaluated by making the change of variable

$$u = \cos \theta, \quad (146)$$

so that it becomes

$$Q_n = \frac{2}{\pi} \sum_{i=1}^N \int_{\cos^{-1}(u_{i+1})}^{\cos^{-1}(u_i)} (c_i + d_i \cos \theta) \cos(n\theta) d\theta. \quad (147)$$

Expansion of the cosine products allows this expression to be rewritten as

$$a_0 = \frac{2}{\pi} \sum_{i=1}^N \int_{\cos^{-1}(u_{i+1})}^{\cos^{-1}(u_i)} (c_i + d_i \cos \theta) d\theta, \quad (148)$$

$$a_1 = \frac{2}{\pi} \sum_{i=1}^N \int_{\cos^{-1}(u_{i+1})}^{\cos^{-1}(u_i)} \left[\frac{1}{2} d_i + c_i \cos \theta + \frac{1}{2} d_i \cos(2\theta) \right] d\theta, \quad (149)$$

and

$$a_n = \frac{2}{\pi} \sum_{i=1}^N \int_{\cos^{-1}(u_{i+1})}^{\cos^{-1}(u_i)} \left\{ \frac{1}{2} d_i \cos[(n-1)\theta] + c_i \cos(n\theta) + \frac{1}{2} d_i \cos[(n+1)\theta] \right\} d\theta, \quad (150)$$

for $n \geq 2$.

Evaluation of the integrals gives

$$a_0 = \frac{2}{\pi} \sum_{i=1}^N \left[c_i \theta + d_i \sin \theta \right]_{\cos^{-1}(u_{i+1})}^{\cos^{-1}(u_i)}, \quad (151)$$

$$a_1 = \frac{2}{\pi} \sum_{i=1}^N \left[\frac{1}{2} d_i \theta + c_i \sin \theta + \frac{1}{4} d_i \sin(2\theta) \right]_{\cos^{-1}(u_{i+1})}^{\cos^{-1}(u_i)}, \quad (152)$$

and

$$a_n = \frac{2}{\pi} \sum_{i=1}^N \left\{ \frac{d_i \sin[(n-1)\theta]}{2(n-1)} + \frac{c_i \sin(n\theta)}{n} + \frac{d_i \sin[(n+1)\theta]}{2(n+1)} \right\}_{\cos^{-1}(u_{i+1})}^{\cos^{-1}(u_i)}, \quad (153)$$

for $n \geq 2$. The Tchebyscheff expansion of this piecewise linear

approximation to $g(u)$ can thus be computed numerically from Eqs. (144), (145), and (151) through (153). The applicability of this method to numeric data is evident. The data points simply become the u_i and $g(u_i)$. If the data are given in graphic or analytic form, the u_i and $g(u_i)$ can be respectively measured or computed.

7. A FORTRAN PROGRAM FOR COMPUTING HARMONIC COEFFICIENTS AND NOISE-TO-SIGNAL RATIOS

In the preceding sections, a method employing the Tchebyscheff expansion was developed for determining the output harmonic coefficients of a nonlinear device. This section describes development of a computer program called henceforth "ODP 11" which uses this method. The program serves as an example of the application of the method and it facilitates the analysis of actual nonlinear characteristics. It can be used to compare characteristics and to determine which portions of a specific characteristic give rise to minimum signal distortions.

From a set of input data points taken from a characteristic, the program computes Tchebyscheff expansions of subregions. The expansions are computed using the method presented in the previous section. The subregions are specified by the user and can correspond to any consecutive subset of the set of input data points. The expansions are computed through an order, not exceeding 9, specified by the user. Input data sets can be taken from characteristics directly or from Hurter-Driffield curves representing photographic processes. When this second option is used, the program automatically transforms the logarithmic data into amplitude transmittance and exposure quantities.

For each subregion, the program output contains the Tchebyscheff expansion coefficients, equivalent noise-to-

signal ratio, and identification data. The program is reproduced in section 11 and a flow chart is shown in Figure 12. The four digit numbers shown in the blocks of the flow chart correspond to the statement numbers of the program.

For each characteristic, the subregions are determined by a list of amplitude parameters and a spacing parameter. These are part of the required program input and correspond numerically to numbers of points of the input data set. Thus, an amplitude parameter of ten corresponds to a region spanned by ten points of the input data set. If the data points are equally spaced, a specific amplitude parameter implies a fixed subregion length. For each amplitude parameter listed, the program varies the location of the subregion by increments corresponding to the spacing parameter. This process is begun at the beginning of the input data set and is continued until the region reaches the end of the set. This process is repeated for each listed amplitude parameter.

For each characteristic ~~input~~, the program input consists of three cards containing parameters followed by data cards. The first parameter card contains identification symbols for the characteristic, a type parameter, the number of points in the data set, the number of amplitude parameters listed, the step parameter, a normalization parameter, and an error parameter. The type parameter is set equal to zero if the function is to be expanded as given. When the type parameter is one, the input data is assumed

to be in the form of a Hurter-Driffield curve. The higher order Tchebyscheff coefficients printed in the output are normalized with respect to the first order if the normalization parameter is one. Otherwise, the coefficients are left unnormalized. The error parameter should be set equal to an estimate of the accuracy of the function values in the input data set. The second parameter card contains a list of the amplitude parameters and the third contains a list of the corresponding orders to which the expansions are to be computed. Each of the cards of the data set contains an argument value followed by the corresponding function value. These cards are read in order of increasing value of the argument.

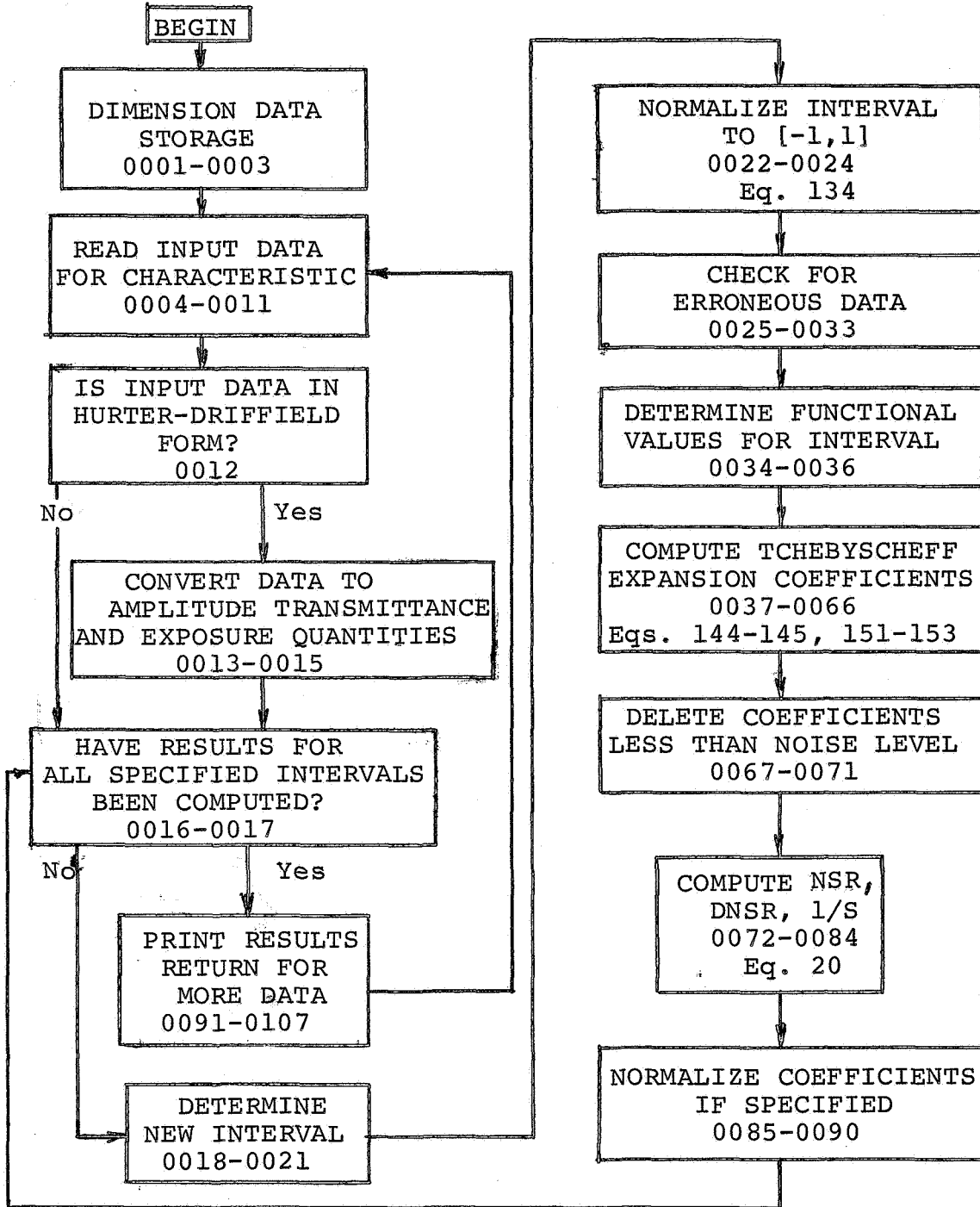


Figure 12. Flow chart for the program ODP-11

8. ANALYSIS OF THE CHARACTERISTIC

CURVES OF TYPE 649-F SPECTROSCOPIC PLATES

The developed fortran program was used to analyze the characteristic curves of Kodak, type 649-F Spectroscopic Plates. This serves as an example of the use of the program outlined in the preceding section. It is also an analysis of the characteristics of plates which are widely used in optical data processing and holography. The results reveal optimum exposure and development conditions for the use of the plates.

The curves were obtained in Hurter-Driffield form from a publication of the Eastman Kodak Company (Kodak, 1967). They represent 10 second exposure to tungsten illumination and development in Kodak developer D-19 at 68° F. Each curve is identified by its corresponding development time. The curves were enlarged photographically to approximately 4" x 8" size. An accurate set of data was then taken from each curve and the corresponding amplitude transmittance vs. exposure data was obtained using a simple fortran program. This data was then accurately plotted on graph paper. The resulting curves are shown in Figure 13. Final data for use in the program was taken from these curves. This procedure allows the final data to be in equal interval form. Thus, a set number of consecutive data points corresponds to a specific region length.

In order to determine the accuracy of the data taking,

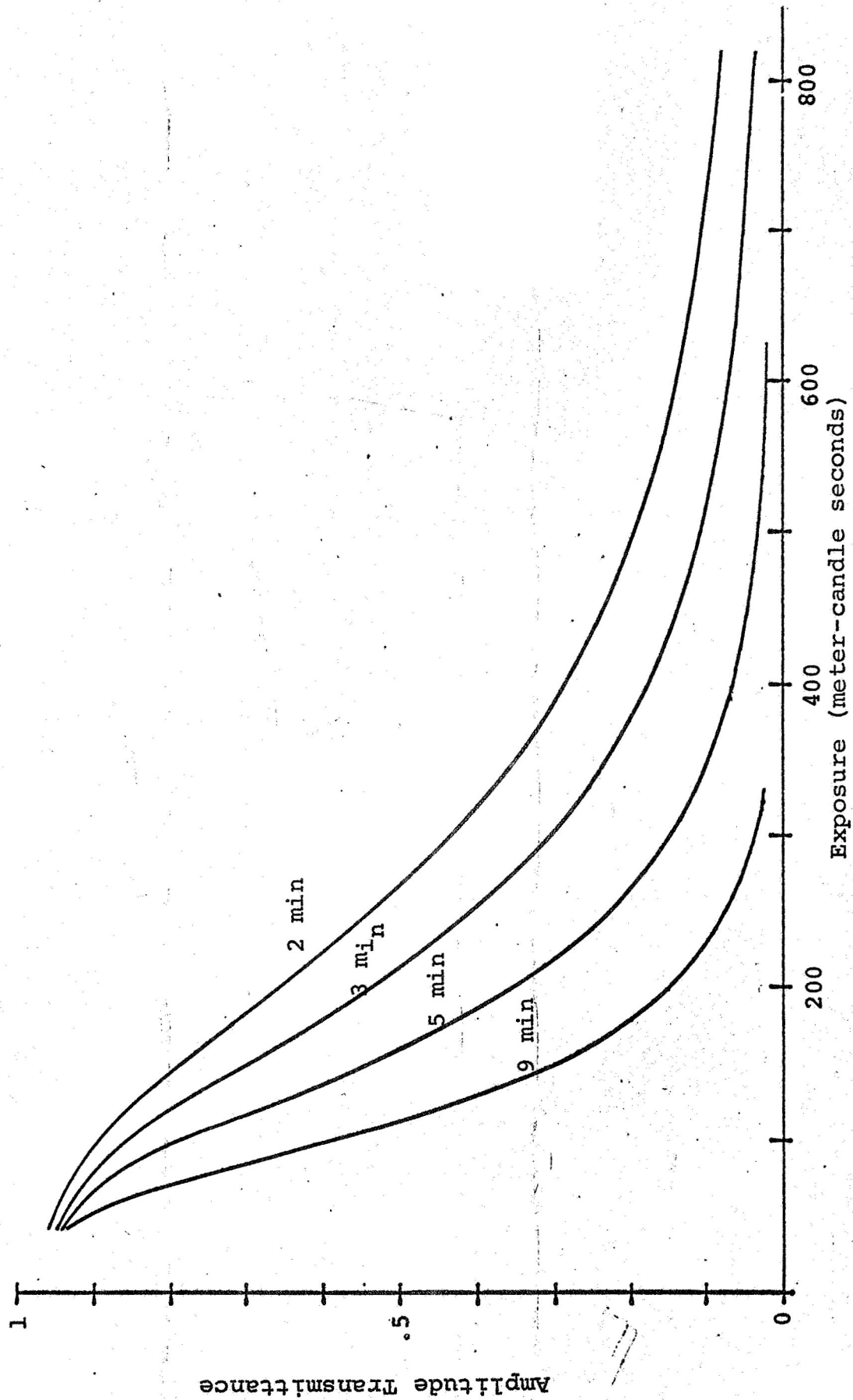


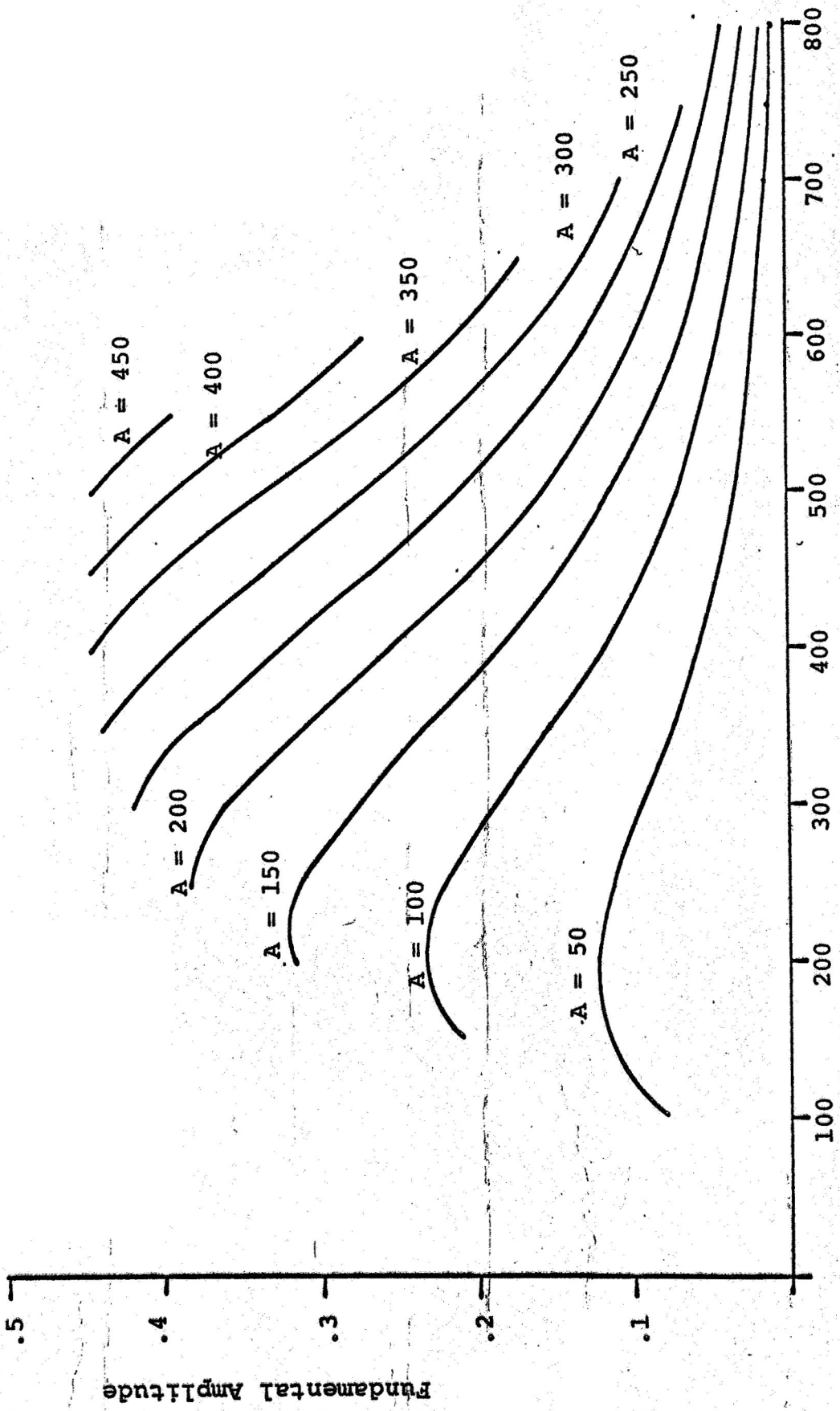
Figure 13. Characteristic curves for type 649-F spectroscopic plates

three independent observations of 96 points on the 2 minute characteristic were made. A short fortran program was then written to estimate the standard deviation of the observations. The resulting estimate was .0033. This standard deviation estimate was subsequently used as the error parameter in the program.

The final data set for each of the 649-F characteristic curves consisted of approximately 90 points. The amplitude parameters used were 11, 21, 31, etc. and the step parameter was 5. Results from the program are shown in Figures 14 through 21. In the figures the input exposure is assumed to be of the form

$$E(x) = E_0 + A \cos(w_x x), \quad (154)$$

where E_0 is the bias level and A is the amplitude of the sinusoid, and w_x represents its spatial radian frequency. Figures 14 through 17 show the output fundamental (undistorted signal) amplitude as a function of bias level and input sinusoid amplitude A . Figures 18 through 21 show the output NSR as a function of bias level and input amplitude.



E_0 , Bias Level

Figure 14. Output fundamental amplitudes for the 2 minute characteristic

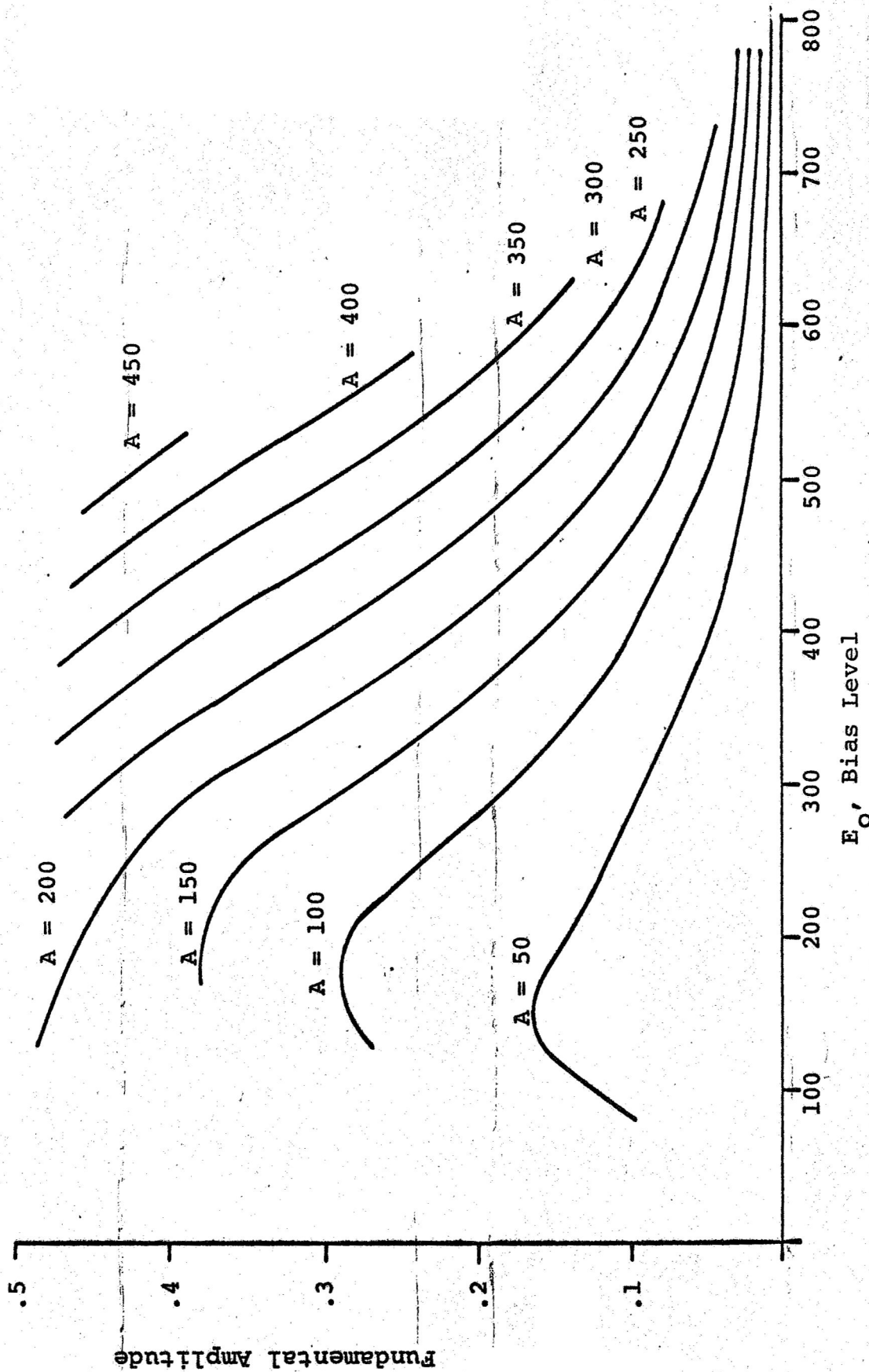


Figure 15. Output fundamental amplitudes for the 3 minute characteristic

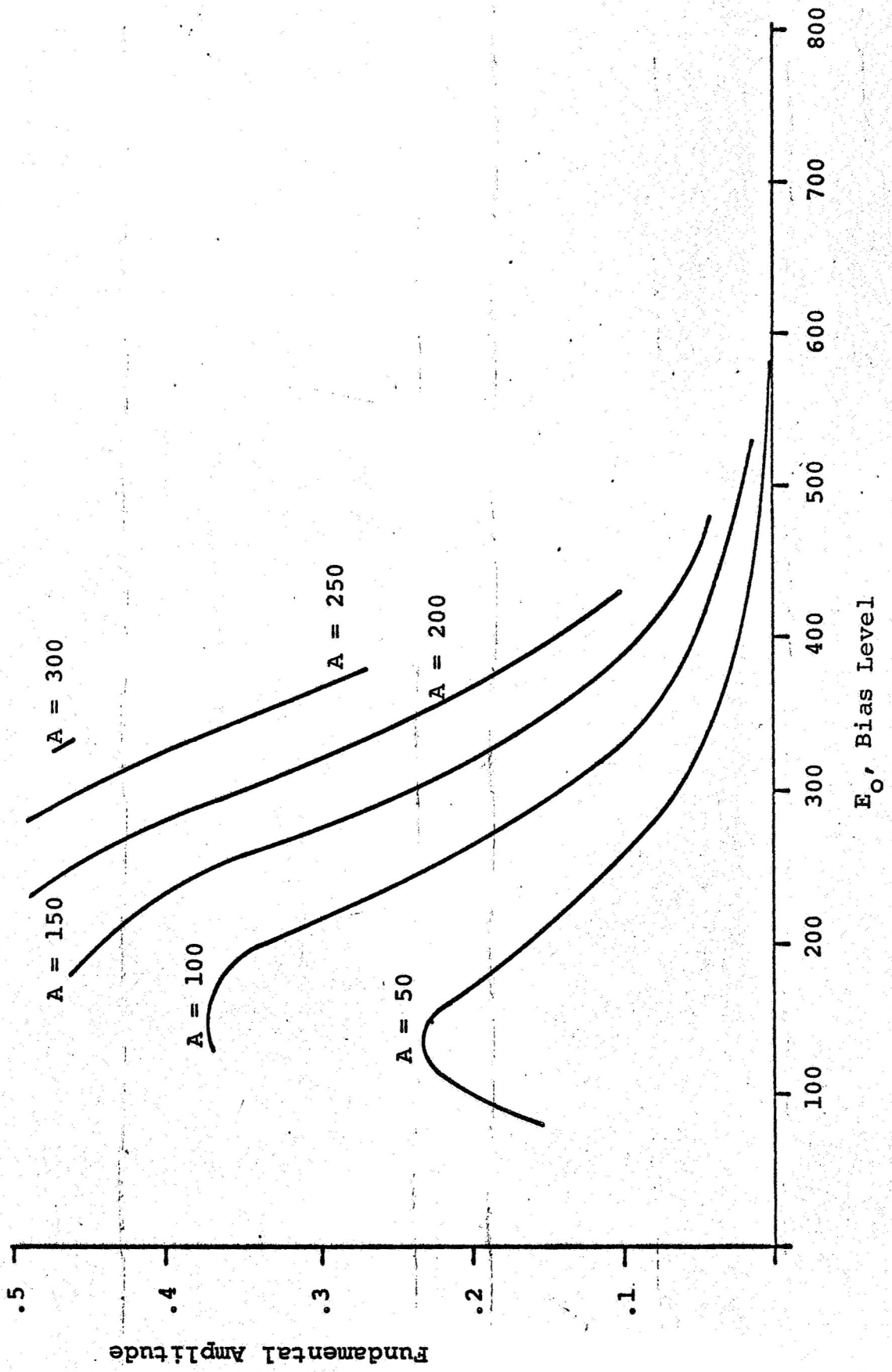


Figure 16. Output fundamental amplitudes for the 5 minute characteristic

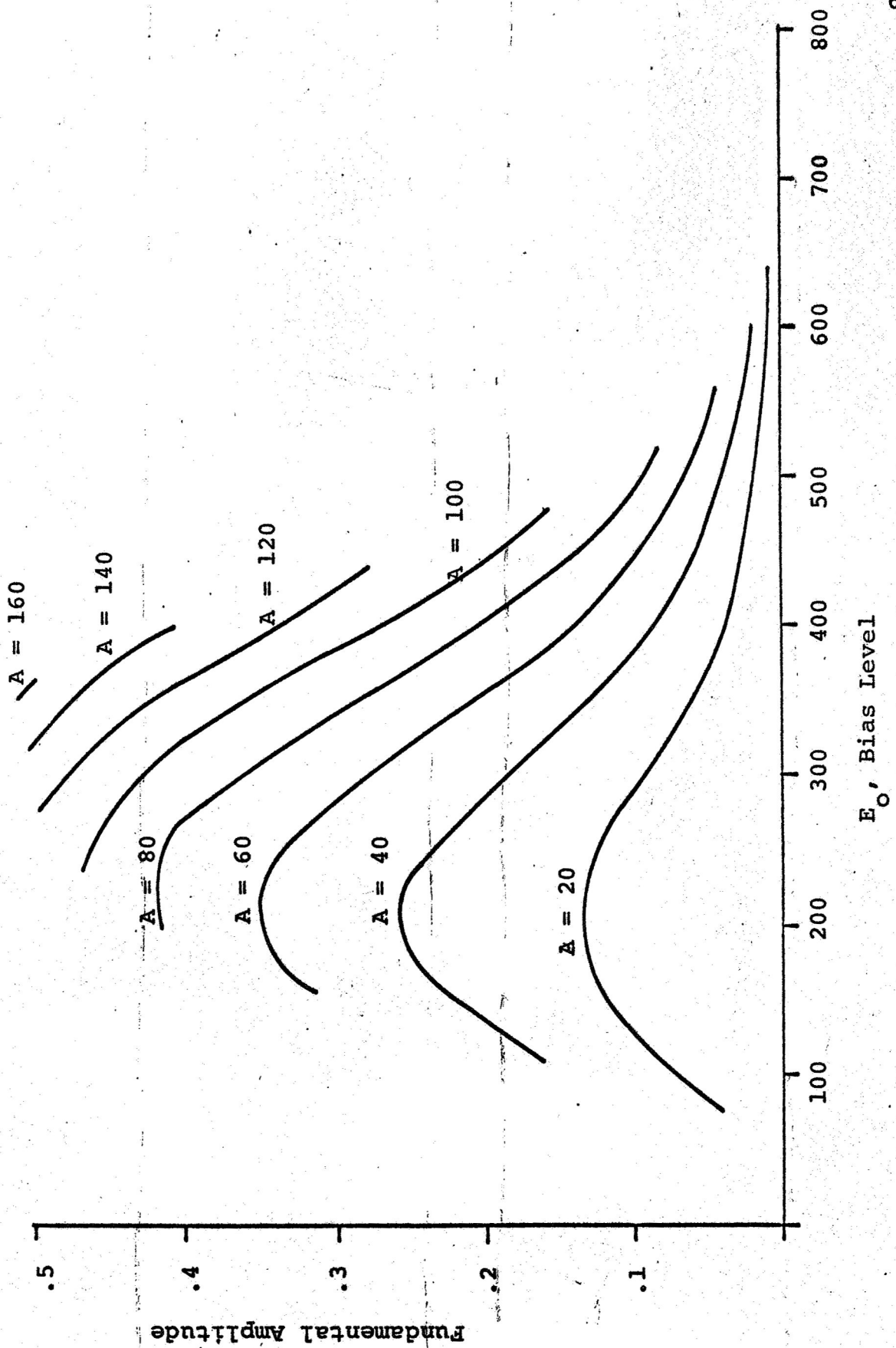
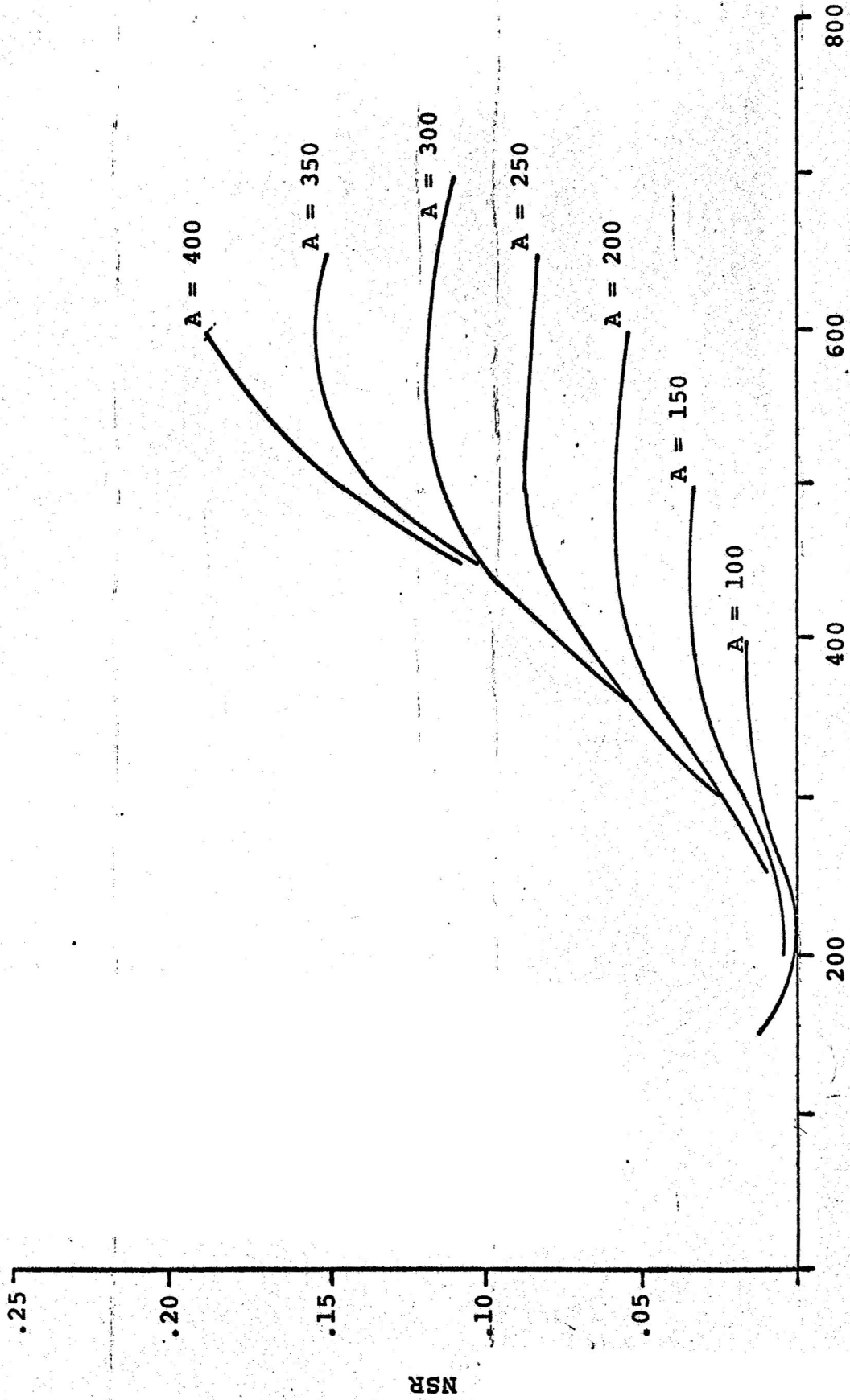


Figure 17. Output fundamental amplitudes for the 9 minute characteristic



E_0 , Bias Level

Figure 18. Noise-to-signal ratios for the 2 minute characteristic

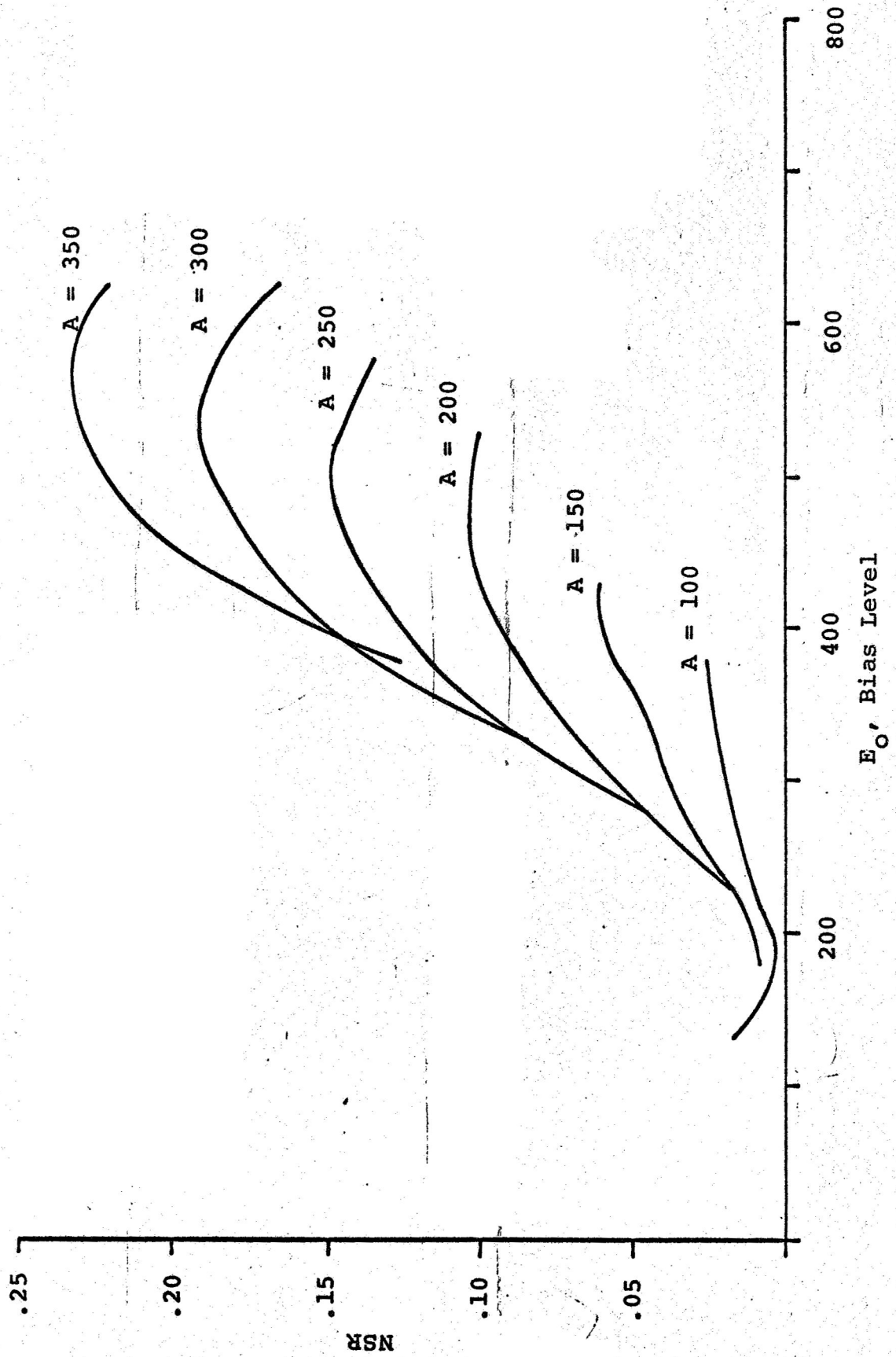


Figure 19. Noise-to-signal ratios for the 3 minute characteristic

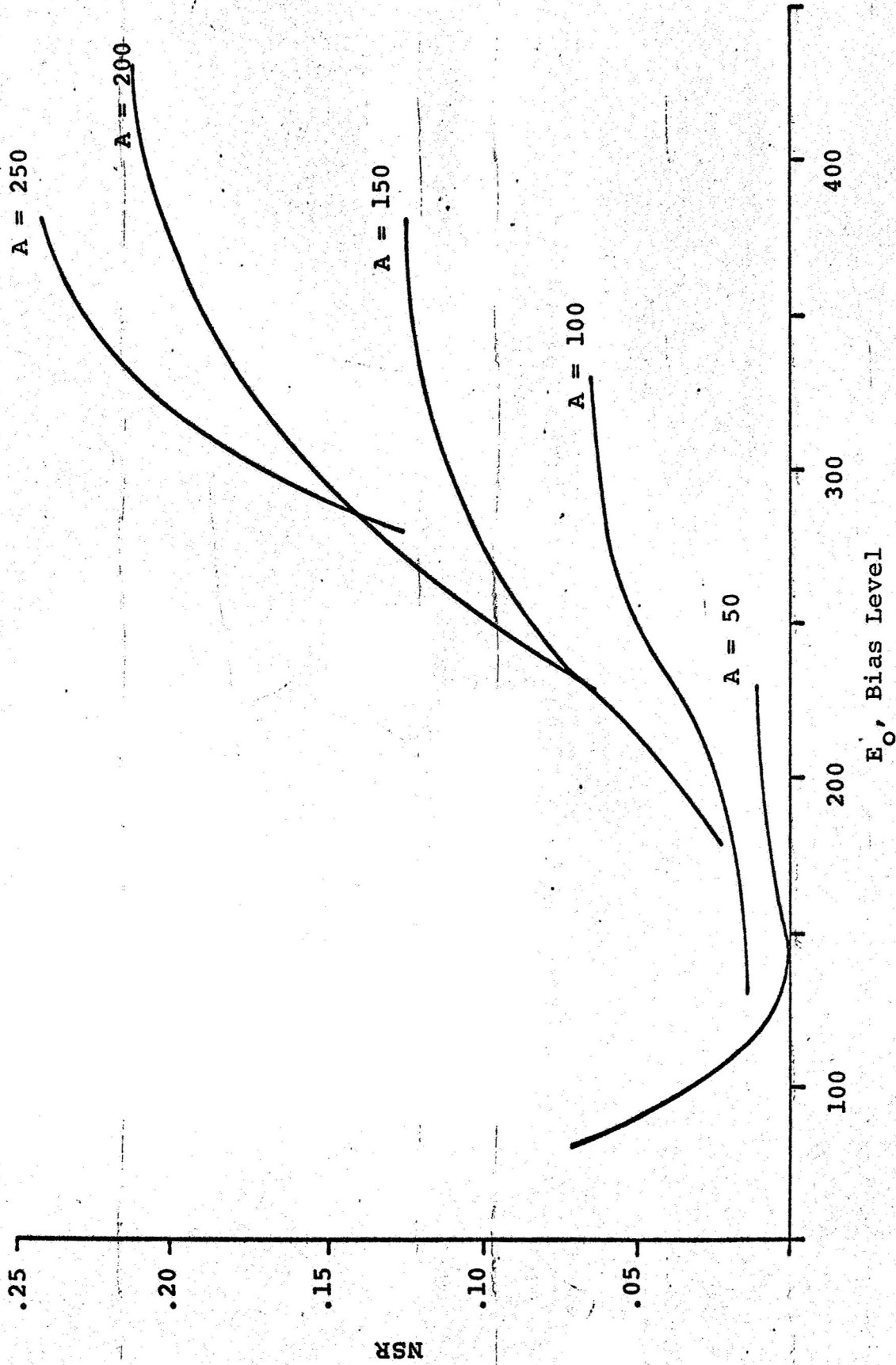


Figure 20. Noise-to-signal ratios for the 5 minute characteristic

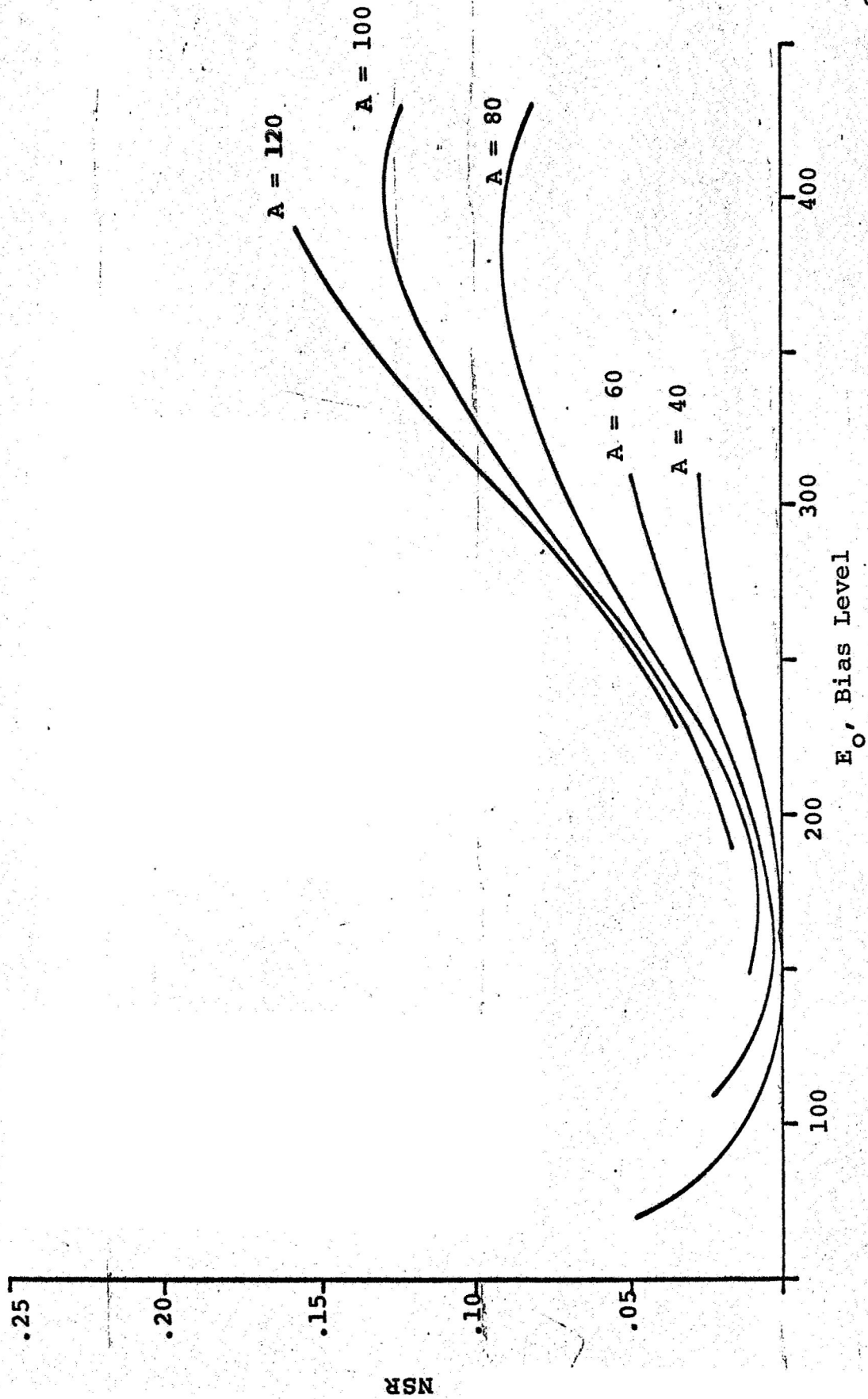


Figure 21. Noise-to-signal ratios for the 9 minute characteristic

9. CONCLUSIONS AND RESULTS

The results of section 5 confirm the theoretical advantages of the Tchebyscheff method in obtaining the output Fourier coefficients of a sinusoidally excited nonlinear device. All of the other expansion methods require higher order terms in order to approximate a given harmonic coefficient. This is also the case for the Fourier series method although significant improvements were obtained by the modification of the expansion procedure (Fourier Series - Method B).

Results of the analysis of the characteristic curves of type 649-F spectroscopic plates show that the effects of the nonlinearities can be minimized for a given characteristic by choosing bias levels appropriate to the amplitude. In most cases, the optimum bias corresponds to the maximization of the output fundamental amplitude. Figure 22 shows the NSR's (at optimum bias) of the four characteristics as a function of this amplitude. From the graph, it can be seen that under optimum-bias conditions the 9 minute characteristic exhibits minimum nonlinear effects. The output fundamental amplitude .4 represents a threshold value. For output amplitudes less than this, all of the characteristics give NSR's less than .02 with optimum bias.

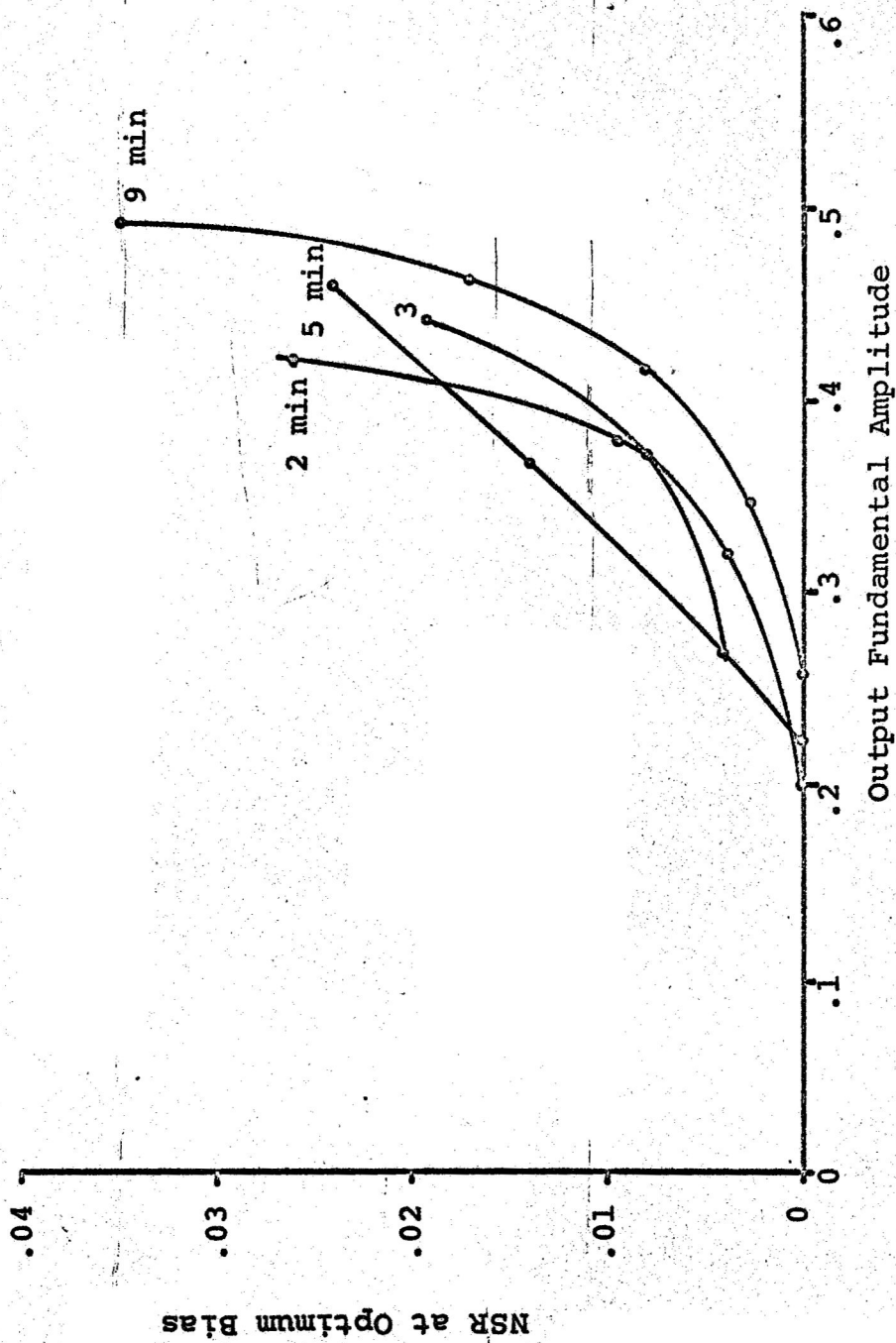


Figure 22. Optimum noise-to-signal ratios for the 649-F characteristic curves

10. LIST OF REFERENCES

- Apostol, T. M. 1957. Mathematical Analysis (A Modern Approach to Advanced Calculus). Addison-Wesley Publishing Company, Inc., Reading.
- Chirlian, P. M. 1965. Analysis and Design of Electronic Circuits. McGraw-Hill Book Company, Inc., New York.
- Davenport, W. B., Jr., and W. L. Root. 1958. Introduction to Random Signals and Noise. McGraw-Hill Book Company, Inc., New York.
- Eastman Kodak Company. 1967. Kodak Data Book P-9. Rochester, New York.
- Espley, D. C. 1933. The Calculation of Harmonic Production in Thermionic Valves with Resistive Loads. Proc. Of I.R.E. 21, 1439.
- Friesem, A. A., and J. S. Zelenka. 1967. Effects of Film Nonlinearities in Holography. Appl. Opt. 6, 1755-1759.
- Jackson, D. 1941. Fourier Series and Orthogonal Polynomials. The Mathematical Association of America, Menasha, Wisconsin.
- Kaplan, W. 1952. Advanced Calculus. Addison-Wesley Publishing Company, Inc., Reading.
- Kozma, A. 1966. Photographic Recording of Spatially Modulated Coherent Light. J. Opt. Soc. Am. 56, 428-432.
- Lamberts, R. L. 1961. Sine-Wave Response Techniques in Photographic Printing. J. Opt. Soc. Am. 51, 982-987.
- Lanczos, C. 1966. Discourse on Fourier Series. Hafner Publishing Company, New York.
- Little, R. E. 1966. The Suppression of Harmonic Distortion in Photographic Images. Optica Acta 13, 31-40.
- Mangulis, V. 1965. Handbook of Series for Scientists and Engineers. Academic Press, New York.
- Middleton, D. 1960. An Introduction to Statistical Communication Theory. McGraw-Hill Book Company, Inc., New York.
- Rochelle, R. W. 1963. Pulse-Frequency-Modulation Telemetry, Thesis, University of Maryland, Dept. of Elec. Engrg., College Park, Maryland.

LIST OF REFERENCES (Continued)

- Ryder, J. D. 1964. Electronic Fundamentals and Applications. Third Edition. Prentice-Hall Inc., Englewood Cliffs, New Jersey.
- Schwartz, M. 1959. Information Transmission, Modulation, and Noise. McGraw-Hill Book Company, Inc., New York.
- Snyder, M. A. 1966. Chebyshev Methods in Numerical Approximation. Prentice-Hall Inc., Englewood Cliffs, New Jersey.
- Tischer, F. J. 1967. Consideration of Nonlinear Effects by Tchebyscheff's Polynomials. NASA Progress Report NGR-34-002-038/S1, Washington, D. C.
- Wilczynski, J. S. 1961. Some Properties of Photographic Image REcording. Proc. Phys. Soc. (London) 77, 17-35.

11. COMPUTER PROGRAM

```

C      ODP11:  NONLINEAR CHARACTERISTIC ANALYSIS
C              PROGRAM
0001      DIMENSION NP(15),NORD(15),X(105),YIN(105),
0002      XN(105),AT(15,105,10)
0003      DIMENSION Y(105),XO(15,105),LSAVE(105),FER(15,
105),SNR(15,105)
C      DIMENSION ERPS(15,105)
C
C      READ INPUT DATA
C
0004      500 READ(1,20) PR,PR1,PR2,NTYPE,N,NAMP,NSTEP,NORM
,ERR
0005      20 FORMAT(2A4,A2,5I5,F10,4)
0006      READ(1,21) (NP(I),I=1,NAMP)
0007      READ(1,21) (NORD(I),I=1,NAMP)
0008      21 FORMAT(20I5)
C
C      PR= IDENTIFICATION SYMBOLS
C      NTYPE=0=INPUT DATA IS FUNCTION TO BE EXPANDED
C      NTYPE=1=INPUT DATA IS IN HURTER-DRIFFIELD FORM
C      N=NUMBER OF DATA POINTS
C      NAMP=NUMBER OF AMPLITUDES
C      NSTEP=NUMBER OF INTERVALS IN STEP
C      NORM=0=COEFFICIENTS ARE PRINTED
C      NORM=1=HIGHER ORDER COEFFICIENTS ARE NORMALIZED
C      TO FIRST ORDER
C      ERR=NOISE LEVEL OF DATA (SET=0 IF NOT USED)
C      NP(I)= NUMBER OF POINTS IN ITH AMPLITUDE
C      NORD(I)= HIGHEST ORDER TO BE FITTED TO ITH
C      AMPLITUDE
C
0009      DO 1 I=1,N
0010      1 READ(1,22) X(I), YIN(I)
0011      22 FORMAT(2F10.4)
0012      IF (NTYPE-1) 30,31,30
0013      31 DO 32 I=1,N
0014      X(I)=10.**X(I)
0015      32 YIN(I)=10.**(-YIN(I)/2.)
C
C      X=EXPOSURE VARIABLE
C      YIN=DENSITY VARIABLE
C
C      DETERMINE LOCAL INTERVALS
C
0016      30 DO 9 K=1,NAMP
0017      DO 8 L=1,N
0018      NP1=NP(K)

```

COMPUTER PROGRAM (Continued)

```

0019          NB=(L-1)*NSTEP+1
0020          NE=NB+NP(K)-1
0021          IF(NE-N) 3,3,9
          C
          C      NORMALIZE LOCAL INTERVAL TO (-1,1)
          C
0022          3 DO 2 I=NB,NE
0023          NUM1=I-NB+1
0024          2 XN(NUM1)=(2.*X(I)-X(NE)-X(NB))/(X(NE)-X(NB))
          C
          C      SEARCH FOR XN OUTSIDE (-1,1)
0025          DO 201 I=1,NP1
0026          IF (1.-XN(I)*XN(I)) 200,201,201
0027          200 WRITE (e,202) I,XN(I),L,K
0028          202 FORMAT (' ',XN(' ,I3,')=' ,E11.4,' IN LINE', '
          OF AMPLITUDE',I3)
0029          IF(XN(I)) 203,203,204
0030          204 XN(I)=.999999
0031          GO TO 201
0032          203 XN(I)=-.999999
0033          201 CONTINUE
          C
          C      ADJUST Y VALUES
          C
0034          DO 4 J=1,NP1
0035          NUM2=NB+J-1
0036          4Y(J)=YIN(NUM2)
          C
          C      COMPUTE EXPANSION
          C
0037          M=NORD(K)+1
0038          DO 5 I=1,M
0039          N1=NP(K)-1
0040          AT(K,L,I)=0.
          C
          C      AT(K,L,I)= TCHEB COEFF FOR AMP(K), INTERVAL(L)
          C      ,ORDER+1=I
          C
0041          I1=I-1
0042          I2=I-2
          C
0043          D( 60 J=1,N1
0044          IF(XN(J)) 301,100,101
0045          301 ARG1=ATAN(SQRT(1.-XN(J)*XN(J))/XN(J))+3.
          1415926
0046          GO TO 104
0047          100 ARG1=1.5707963
0048          GO TO 104
0049          101 ARG1=ATAN(SQRT(1.-XN(J)*XN(J))/XN(J))
0050          104 IF(XN(J+1)) 303,102,103

```

COMPUTER PROGRAM (Continued)

```

0051      303 ARG2=ATAN(SQRT(1.-XN(J+1)*XN(J+1))/XN(J+1))
          +3.1415926
0052      GO TO 105
0053      102 ARG2=1.5707963
0054      GO TO 105
0055      103 ARG2=ATAN(SQRT(1.-XN(J+1)*XN(J+1))/XN(J+1))
0056      105 AO=(Y(J)*XN(J+1)-Y(J+1)*XN(J))/(XN(J+1)-XN(J))
0057      A1=(Y(J+1)-Y(J))/(XN(J+1)-XN(J))
0058      IF (I-2) 107,108,109
0059      107 AT(K,L,I)=AT(K,L,I)+(AO*(ARG1-ARG2)+A1*(SIN(
          ARG2)))
0060      GO TO 60
0061      108 AT(K,L,I)=AT(K,L,I)+(.5*A1*(ARG1-ARG2)+AO*(
          SIN(ARG1)-SIN(ARG2))+1.25*A1*(SIN(2.*ARG1)-
          SIN(2.*ARG2)))
0062      GO TO 60
0063      109 AT(K,L,I)=AT(K,L,I)+(.5*A1*(SIN(I2*ARG1)-SIN
          (I2*ARG2)))/I2
          1+AO*(SIN(I1*ARG1)-SIN(I1*ARG2))/I1
          2+.4*A1*(SIN(I*ARG1)-SIN(I*ARG2))/I)
0064      60 CONTINUE
0065      5 AT(K,L,I)=AT(K,L,I)/1.5707963
0066      XO(K,L)=.5*(X(NB)+X(NE))
          C
          C      CHECK FOR COEFFICIENTS LESS THAN NOISE LEVEL
          C
0067      DO 7 I=1,M
0068      ATAB=ABS(AT(K,L,I))
0069      IF (ATAB-ERR) 6,7,7
0070      6 AT(K,L,I)=0.0
0071      7 CONTINUE
          C
          C      COMPUTE NSR,1/S
          C
          C      ERPS(K,L)=ESTIMATE OF NUMERICAL ERROR IN FER(K,L)
          C      SNR(K,L)=RECIPROCAL OF SQUARED FUNDAMENTAL
          C      AMPLITUDE
          C      FER(K,L)=NOISE TO SIGNAL RATIO
0072      SIG2=AT(K,L,2)*AT(K,L,2)
0073      HAR2=0.0
0074      DO 13 I=3,M
0075      13 HAR2=HAR2+AT(K,L,I)*AT(K,L,I)
0076      IF(SIG2) 15,14,15
0077      14 FER(K,L)=0.0
0078      ERPS(K,L)=0.0
0079      SNR(K,L)=0.0
0080      GO TO 8
0081      15 FER(K,L)=HAR2/SIG2
0082      SNR(K,L)=1./SIG2
0083      ERR1=ERR*ERR

```

COMPUTER PROGRAM (Continued)

```

0084          ERPS(K,L)=ERR1/SIG2
      C
      C      NORMALIZE COEFFICIENTS IF SPECIFIED
      C
0085          IF (NORM-1) 8,18,8
0086          18 IF (AT(K,L,2)) 16,8,16
0087          16 DO 17 I=3,M
0088          17 AT(K,L,I)=AT(K,L,I)/AT(K,L,2)
0089          8 LSAVE(K)=L
0090          9 CONTINUE

      C
      C      WRITE RESULTS
      C
0091          DO 11 I=1,NAMP
0092          NUM3=NP(I)
0093          AMP=X(NUM3)-X(1)
0094          WRITE(3,24) PR,PR1,PR2,N,NP(I),NORM,ERR
0095          24 FORMAT('1',2A4,A2,' N=',I3,' NP=',I3,' NORM=',
      I2,' ERR=',E10.3)
0096          WRITE(3,25)
0097          25 FORMAT(' ','NB',4X,'XZRO',5X,'XINT',5X,
      'YINT',5X,'NSR',9X,
      1'DNSR',8X,'1/S',9X,'TCHEBYSCHIEFF EXPANSION
      COEFFICIENTS')
0098          MM=NORD(I)+1
0099          LS=LSAVE(I)
0100          DO 11 J=1,LS
0101          NB=(J-1)*NSTEP+1
0102          NE=NB+NP(I)-1
0103          XINT=X(NE)-X(NB)
0104          YINT=YIN(NE)-YIN(NB)
0105          11 WRITE(3,26) NB,XO(I,J),XINT,YINT,FER(I,J),
      SNR(I,J),
      1(AT(I,J,K),K=1,MM)
0106          26 FORMAT('0',I3,1X,3F9.3,1X,8(E11.4,1X)/69X,
      5(E11.4,1X))
0107          GO TO 500
0108          END

```